



Mohamed Khider University of Biskra
Faculty of Science and Technology
Department of Electrical Engineering

MASTER'S THESIS

Science and Technology
Telecommunications
Networking

Ref.:

Presented and defended by:

Azizi Moaz Abdel Khalek

Sunday 1 June 2025

Study of spatial consistency parameters effects on 5G communication systems

Supervisor:
Dr. ABDESSELAM Salim

Committee:

Mr. Ameid sofiane	MAA	University Of Biskra	President
Mr. Boukredine Salah eddine	MAA	University Of Biskra	Examiner
Dr. ABDESSELAM Salim	MCB	University Of Biskra	Supervisor

Academic Year: 2024/2025

Acknowledgment

First and foremost, we would like to express our gratitude to God, the Almighty, for bestowing upon us the strength, determination, and patience throughout our years of study.

We extend our heartfelt thanks to our promoter professor “**Salim Abdesselam**”, for their willingness to supervise us, and for their guidance, encouragement, and advice. We are also grateful to the president of the jury doctor “**Ameid sofiane** ” for their agreement to evaluate our work. We would like to express our appreciation to Examiner of the jury doctor “**Boukredine Salah eddine**”, for agreeing to chair our defense jury. Our sincere thanks and gratitude go out to all the teachers who have contributed to our undergraduate and postgraduate education at our faculty, our unalterable respect towards the teachers of electrical networks Lastly, we would like to thank all the individuals who have offered us their encouragement and support, both near and far, during the completion of this work.

Your support has been invaluable.

DEDICATION

In the name of Allah, the Most Compassionate, the Most Merciful, This work is a tapestry woven with threads of love, resilience, and shared memories. It unfurls across generations, binding us together in a symphony of familial bonds. My mother, Fatima: Her unwavering faith, like the ancient roots of a tree, has anchored our family. Her love, a gentle current that flows through our veins, has shaped my very being. My dear father, Mouhamed El Moutaa: His strength, etched into the lines of his weathered hands, has been my compass. His wisdom, whispered in late night conversations, has illuminated my path. My brothers, Mokim, Adel, Adem, Abdou, Mouhamed, Housseem and Malek: They are the pillars of laughter echoing through our home, the guardians of secrets shared under moonlit skies. Their camaraderie, a fortress against life's storms, has steadied me. My sisters, Imane and Sabrina: their kindness, a sunbeam that dances across our days, has painted our memories in hues of warmth. Her laughter, contagious and healing, has stitched joy into the fabric of our existence. and my friends Abdo, Ali, Imed, Zaki, Walid, Salah, Sami, Ridha, and others: You are the ink that colors the margins of my life. Your friendship, a mosaic of shared laughter and late-night conversations, has been my sanctuary. Your belief in me, a lighthouse guiding my ship through tempests, has made this journey worthwhile. May this work be a testament to the mosaic of souls who have touched mine their fingerprints etched on every page. May it resonate with the heartbeat of shared experiences, whispered prayers, and laughter echoing through time. Thank you, dear family, friends, and kindred spirits

Abstract:

This work investigates the influence of spatial consistency on the propagation behavior of 5G millimeter-wave (mmWave) communication systems. Spatial consistency refers to the smooth evolution of channel characteristics as the user moves, such as path loss, delay spread, and angle of arrival. Using the NYUSIM simulator, we conducted simulations under realistic urban microcell conditions at 28 GHz, comparing different shadow fading correlation distances, trajectory shapes (linear and hexagonal), and LOS/NLOS scenarios. The results show that spatial consistency has a significant impact on link stability, beamforming effectiveness, and signal fluctuation. Our findings highlight the importance of including spatial correlation in 5G modeling and suggest practical design recommendations for mmWave network planning.

Keywords: 5G, mmWave, Spatial Consistency, NYUSIM, Channel Modeling, Beamforming, Urban Microcell, Mobility

المخلص:

يهدف هذا العمل إلى دراسة تأثير التناسق المكاني على سلوك الانتشار في أنظمة الاتصالات اللاسلكية للجيل الخامس (5G) باستخدام موجات المليمتر (mmWave). يشير التناسق المكاني إلى التغيير التدريجي والمنظم في خصائص القناة مثل فقدان المسار، وانتشار التأخير، وزاوية الوصول، أثناء حركة المستخدم. تم إجراء محاكاة باستخدام برنامج NYUSIM ضمن بيئة خلوية حضرية عند تردد 28 جيجاهرتز، حيث تمت مقارنة تأثير المسافة الارتباطية لتضاؤل الظل، وأشكال المسار (خطي وسداسي)، وظروف القناة (LOS/NLOS). أظهرت النتائج أن التناسق المكاني له تأثير كبير على ثبات الاتصال، وفعالية التوجيه الشعاعي (Beamforming)، وتقلب الإشارة. وتؤكد النتائج أهمية اعتماد نماذج واقعية تأخذ هذا العامل بعين الاعتبار عند تصميم شبكات الجيل الخامس.

الكلمات المفتاحية: الجيل الخامس، mmWave، التناسق المكاني، NYUSIM، نمذجة القناة، التوجيه الشعاعي، خلوية حضرية، التنقل

Résumé :

Ce mémoire étudie l'influence de la cohérence spatiale sur le comportement de propagation des systèmes de communication 5G à ondes millimétriques (mmWave). La cohérence spatiale désigne l'évolution fluide des caractéristiques du canal telles que la perte de trajet, la dispersion temporelle et l'angle d'arrivée au fur et à mesure que l'utilisateur se déplace. À l'aide du simulateur NYUSIM, nous avons réalisé des simulations dans un environnement urbain réaliste à 28 GHz, en comparant différentes distances de corrélation de l'atténuation d'ombre, des formes de trajectoire (linéaire et hexagonale) et des scénarios LOS/NLOS. Les résultats montrent que la cohérence spatiale a un impact significatif sur la stabilité du lien, l'efficacité du beamforming et la variation du signal. Cette étude souligne l'importance d'intégrer la cohérence spatiale dans la modélisation des réseaux 5G et propose des recommandations pour leur conception.

Mots-clés : 5G, ondes millimétriques, cohérence spatiale, NYUSIM, modélisation du canal, formation de faisceaux, microcellule urbaine, mobilité

Table of content

General Introduction	1
Chapter I: Foundations and Key Technologies of 5G Networks	
I.1 Introduction	2
I.2 Definition of 5G Technology	2
I.3 Evolution from Previous Generations	3
I.4 Key 5G Technologies	5
I.4.1 Millimeter-Wave (mmWave)	5
I.4.2 Multiple Antenna Systems	7
I.4.3 Millimeter Waves: In-Depth Overview	8
I.4.4 Network Slicing	9
I.4.5 Edge Computing	11
I.5 Challenges of 5G	12
I.6 Conclusion	12
Chapter II: Spatial consistency Parameters of the Channel	
II.1 Introduction	13
II.2 Definition of Spatial Consistency	14
II.3 Channel Parameters Affecting Spatial Consistency	14
II.3.1 Path Loss	14
II.3.2 Received Signal Power	15
II.3.3 Power Delay Profile (PDP)	16
II.3.4 Shadow Fading	17
II.3.5 Angle of Arrival (AoA)	18
II.3.6 Angle of Departure (AoD)	19
II.4 Importance of Spatial Consistency in 5G Applications	20
II.4.1 Mobility and Handover Management	20
II.4.2 Beamforming and Beam Tracking	21
II.4.3 Massive MIMO Channel Estimation	22
II.4.4 AR/VR and Low-Latency Applications	22

II.4.5 Vehicular Communication Systems	22
II.5 Conclusion	23
Chapter III: Simulation and Results	
III.1 Introduction	24
III.2 Introduction to NYUSIM Simulator	24
III.3 NYUSIM Simulation Parameters	25
III.3.1 Channel Parameters	25
III.3.2 Antenna Parameters	27
III.3.3 Spatial Consistency Parameters	28
III.4 Parameter Justifications	30
III.4.1 Justification of Channel Parameters	30
III.4.2 Justification of Antenna Parameters	31
III.4.3 Spatial Consistency Parameter Choices	32
III.5 Simulations and Results	32
III.5.1 Simulation Setup	33
III.5.2 Scenario One: LOS – Linear Track	33
III.5.3 Scenario Two: NLOS – Linear Track	38
III.5.4 Scenario Three: LOS – Hexagonal Track	41
III.5.5 Scenario Four: NLOS – Hexagonal Track	45
III.5.6 Comparative Summary Table	43
III.6 Conclusion	50
General Conclusion	51
References	

List of Figures

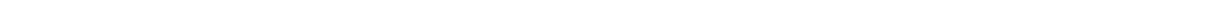
Figure I.1: Smart City	6
Figure I.2: The Evolution of Mobile Network Generations	7
Figure I.3: Atmospheric Absorption in mmWave Bands	9
Figure I.4: Millimeter-Wave Range	11
Figure I.5: Illustration of SISO, SIMO, MISO, MIMO	13
Figure I.6: Coverage Comparison Between Legacy Antenna and Massive MIMO	14
Figure I.7: 5G Network Slicing Categories: eMBB, URLLC, and mMTC	11
Figure I.8: Edge Computing Role in the 5G Network	12
Figure II.1: 5G Base Station Environments	14
Figure II.2: Showcase of Path Loss	15
Figure II.3: Shadow Fading Impact	17
Figure II.4: Signals With and Without Shadow Fading	18
Figure II.5: Angle of Arrival Demonstration	18
Figure II.6: Angle of Departure Demonstration	19
Figure II.7: 5G Handover Graph	20
Figure II.8: Beam Outage vs Wind Speed	21
Figure II.9: Spatial Correlation Function in Vehicular MIMO	22
Figure III.1: GUI of NYUSIM	25
Figure III.2: Types of Base Stations	25
Figure III.3: Omnidirectional PDP for scenario 1	34
Figure III.4: directional PDP for scenario 1	34
Figure III.5: User terminal track in SF map for scenario 1	35
Figure III.6: intensity map of spatially correlated SF for scenario 1	36
Figure III.7: channel parameters.	29
Figure III.8: channel parameters.	29
Figure III.9: channel parameters.	30
Figure III.10: antenna parameters.	31
Figure III.11: special consistency parameters.	32
Figure III.12: Map of spatially correlated LOS condition for scenario 1	37
Figure III.13: directional PDP for scenario 2	38
Figure III.14: omnidirectional PDP for scenario 2	39
Figure III.15: User terminal track in SF map for scenario 2	39
Figure III.16: intensity map of spatially correlated SF for scenario 2	40
Figure III.17: Map of spatially correlated LOS condition for scenario2	40
Figure III.18: directional PDP for scenario 3	42
Figure III.19: omnidirectional PDP for scenario 3	43
Figure III.20: User terminal track in SF map for scenario 3	43
Figure III.21: Intensity map of spatially correlated SF for scenario 3	44
Figure III.22: Map of spatially correlated LOS condition for scenario 3	44
Figure III.23: directional PDP for scenario 4	46

Figure III.24: omnidirectional PDP for scenario 4	46
Figure III.25: User terminal track in SF map for scenario 4	47
Figure III.26: Intensity map of spatially correlated SF	47
Figure III.27: Map of spatially correlated LOS condition	48
Figure III.28: omnidirectional PDP	49
Figure III.29: User terminal scenario 4	51
Figure III.30: Map of spatially correlated LOS for scenario 4	53
Figure III.31:PDP graphs of simulation with and without special consistency	55

List of Tables

Table I.1: Comparison of the Different Generations	4
Table III.1: Typical Climatic Conditions in Biskra, Algeria	30
Table III.2: Parameters Used for Scenario One	33
Table III.3: Observation of Scenario One	37
Table III.4: Parameters Used for Scenario Two	38
Table III.5: Observation of Scenario Two	41
Table III.6: Parameters Used for Scenario Three	42
Table III.7: Observation of Scenario Three	45
Table III.8: Parameters Used for Scenario Four	46
Table III.9: Observation of Scenario Four	48
Table III.10: Comparative Overview of Simulation Outcomes	49

General introduction



General introduction

Wireless communication has transformed dramatically over the past few decades what started as simple voice transmission in the 1G era has grown into the powerful and interconnected world we live in today. Now, with the emergence of Fifth Generation (5G) networks, we stand on the threshold of a new revolution. Unlike previous generations that mainly improved speed and capacity, 5G introduces a rich ecosystem of technologies designed to enable real-time responsiveness, ultra-high reliability, and massive device connectivity all of which are essential for smart cities, autonomous vehicles, remote surgeries, and next-generation industrial systems.

This thesis is structured around three chapters, each designed to build a deeper understanding of how 5G functions and how its performance can be evaluated and optimized.

Chapter 1 provides a general overview of 5G technology, its evolution from previous generations, and the key technologies that support its performance including millimeter-wave (mmWave) communication, massive MIMO antenna systems, network slicing, and edge computing. This chapter also outlines the new challenges introduced by 5G, particularly in modeling high-frequency wireless channels accurately.

Chapter 2 dives into the theoretical foundations of one of the most critical aspects of modern channel modeling: spatial consistency. This chapter explains how different physical parameters such as path loss, received signal power, and delay profiles must evolve smoothly as users move through space. Special attention is given to how spatial consistency influences advanced antenna systems like MIMO.

Chapter 3 presents a simulation-based study using the NYUSIM channel simulator to analyze the impact of spatial consistency on 5G system performance. Through carefully controlled simulations, we investigate how various channel parameters behave in real-world conditions, providing insights into how spatial modeling can improve the realism and accuracy of 5G network design.

In summary, this thesis combines technical analysis with simulation experiments to explore how spatial consistency plays a vital role in ensuring 5G networks deliver on their promise both now and in future wireless systems

Chapter I: Foundations and Key Technologies of 5G Networks

Chapter I

Foundations and key technologies of 5G networks

I.1 Introduction

Wireless communication has come a long way over the past few decades, and today, we stand at the forefront of a new era with the arrival of 5G — the fifth generation of mobile networks. Unlike previous generations, which mainly focused on increasing data speeds, 5G brings a complete overhaul of mobile communication, aiming to support a wide range of new technologies and services. From autonomous vehicles and smart cities to remote surgeries and the Internet of Things (IoT), 5G is expected to be the backbone of a more connected and intelligent world.

In this chapter, we present a general overview of 5G technology, highlighting its key features, evolution, use cases, and the concept of spatial consistency, which plays a crucial role in accurate modeling and simulation of 5G communication systems.

I.2 Definition of 5G technology

The Fifth Generation (5G) of wireless communication marks a major step forward in how we connect and interact with the world around us. Unlike previous generations that focused mainly on faster internet or clearer calls, 5G brings a powerful, flexible platform capable of supporting a wide range of smart technologies. Its ultra-low latency allows for instant communication, which is essential for things like self-driving cars, remote surgeries, and advanced industrial systems. In the context of smart cities like the one illustrated in the figure I.1 5G plays a central role in linking smart mobility, traffic control, utility management, and connected homes. It also supports essential services such as healthcare, public safety, and environmental monitoring. By enabling seamless interaction between vehicles, wearables, and smart devices, 5G helps create safer, more efficient, and more responsive urban environments. It's more than just faster internet it's the foundation of future city living.



Figure I.1: Smart city. [1]

It is structured around three primary service domains: enhanced mobile broadband (eMBB), ultra-reliable low-latency communications (URLLC), and massive machine-type communications (mMTC). eMBB enables high-speed services like ultra-HD streaming and virtual reality. URLLC supports applications such as autonomous vehicles and remote medical procedures, requiring minimal latency and high reliability. mMTC provides scalable connectivity for massive IoT systems in smart cities and industries.

These capabilities are powered by cutting-edge technologies such as millimeter-wave (mmWave) spectrum, massive MIMO antenna systems, network slicing, and edge computing. Together, they make 5G not just a communication upgrade, but the foundation for the Fourth Industrial Revolution.[2]

I.3 Evolution from previous generations

The evolution from 1G to 5G represents over four decades of continuous innovation in mobile communications, with each generation addressing the limitations of its predecessor while introducing new capabilities, as explained in the table below:

Table I 1: Comparison of the different generations.

Generation	Era	Technology	Key Features	Typical Speeds	Main Limitations
1G	1980s	Analog (AMPS, TACS, NMT)	Voice-only, no encryption, limited capacity	~2.4 kbps	Poor security, no data services, low voice quality
2G	1990s	Digital (GSM, CDMA)	SMS, circuit-switched data, caller ID, basic encryption	~64 kbps	Very limited internet (WAP), slow data speeds
3G	2000s	Packet-switched	Mobile internet, email, video calls, mobile TV, smartphone support	~2 Mbps	Insufficient for high-bandwidth apps
4G/LTE	2010s	All-IP, OFDMA, MIMO	HD streaming, low latency, cloud computing	100 Mbps – 1 Gbps	Limited support for massive IoT and ultra-low latency
5G	2020s	New radio, mmWave, Network slicing.	Ultra-low latency, high speed, energy efficient, massive IoT, critical comms support	1–10 Gbps+	Requires dense infrastructure, rollout still ongoing

Each generation of wireless technology has built on the last, solving new challenges and unlocking fresh possibilities, as shown in figure I.2 illustrating their evolution. But 5G isn't just another step forward it's a revolution. Unlike past upgrades, 5G completely reimagines how networks function, making them flexible enough to handle everything from smart factories to remote surgery, all at once.[2]

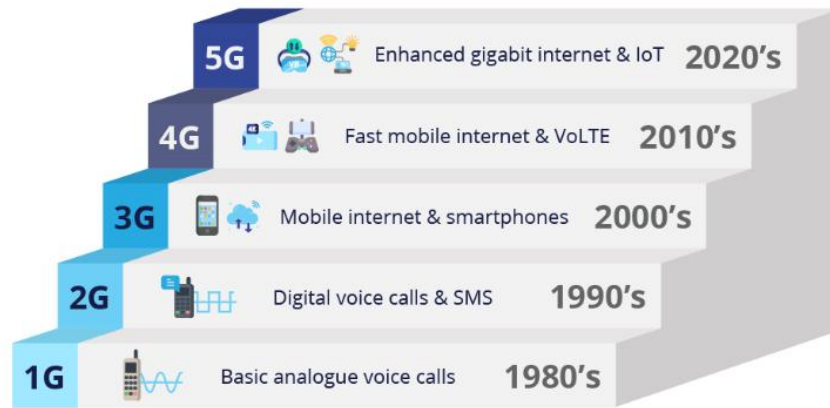


Figure I 2: The evolution of mobile network generations [3]

I.4 Key 5G Technologies

5G relies on a set of advanced technologies that enable higher data rates, lower latency, and improved connectivity, forming the foundation for next-generation mobile communication.

I.4.1 Millimeter-wave (mmWave)

Millimeter waves (mmWave) refer to the portion of the electromagnetic spectrum with frequencies typically ranging from 24 GHz to 100 GHz, corresponding to wavelengths between 1 mm and 10 mm. These high-frequency bands are a core component of 5G technology due to their ability to support extremely high data rates, thanks to the availability of wide bandwidth channels ranging from hundreds of MHz to several GHz [4].

However, mmWave propagation faces several physical limitations. One of the main challenges is atmospheric absorption, which is primarily caused by oxygen and water vapor molecules. For instance, significant signal attenuation occurs around 60 GHz due to oxygen absorption, and at approximately 22 GHz and 183 GHz due to water vapor as we can see in figure (I.3). These losses greatly reduce transmission range, especially in humid environments [6]. Furthermore, mmWave signals are highly sensitive to weather conditions such as rain, fog, snow, and even humidity. These factors can result in substantial signal degradation.

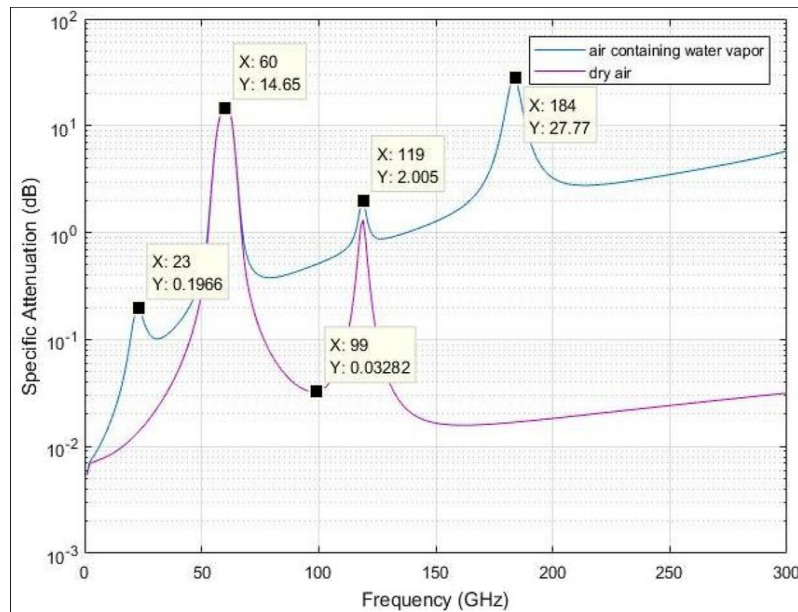


Figure I 3: Atmospheric absorption in mmWave bands [5]

Physical obstructions like buildings, foliage, or even the human body can block or significantly weaken mmWave signals. Unlike the lower frequency bands used in earlier generations (e.g., 3G or 4G), mmWave signals do not easily penetrate solid objects. To overcome this limitation, advanced beamforming techniques and dense small-cell deployments are required, with base stations placed every 100–200 meters in urban areas to maintain continuous coverage [4].

Regarding propagation mechanisms, mmWave signals primarily rely on line-of-sight (LoS) transmission but can also utilize phenomena like reflection, scattering, and diffraction. However, due to their short wavelength, diffraction is extremely limited, which means that mmWave signals struggle to bend around corners or obstacles. Reflective surfaces such as glass or metal can help maintain the link through indirect paths, though often at reduced signal strength [4].

In summary, while mmWave offers immense potential in terms of data throughput and user density, it introduces significant technical challenges due to its propagation characteristics. Effective 5G network design must therefore account for these limitations by deploying dense infrastructure and implementing intelligent signal management and compensation strategies.

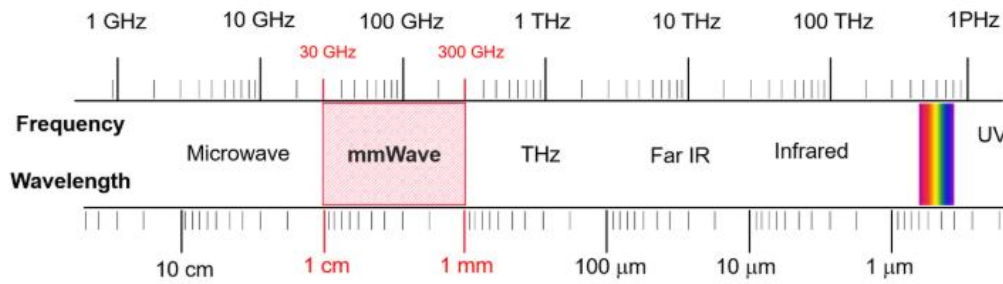


Figure I.4: Millimeter-wave range [6]

I.4.2 Multiple Antenna Systems

I.4.2.1 SISO (Single Input Single Output) is the simplest antenna configuration, where both the transmitter and the receiver use only one antenna. It was used in early wireless systems such as 1G and 2G. While SISO is easy to implement, it has limited performance and no spatial diversity, making it vulnerable to fading and interference [7].

I.4.2.2 SIMO (Single Input Multiple Output) involves one transmitting antenna and multiple receiving antennas. This setup improves signal quality and reliability through diversity reception, as the receiver can select or combine signals from different paths to mitigate fading. SIMO is often used in uplink scenarios where mobile devices have one antenna and base stations have several [7].

I.4.2.3 MISO (Multiple Input Single Output) consists of multiple antennas at the transmitter and a single antenna at the receiver. It allows the transmitter to apply beamforming, focusing the signal toward the user to improve range and reduce interference. MISO is typically used in downlink channels in modern wireless networks [7].

I.4.2.4 MIMO (Multiple Input Multiple Output) employs multiple antennas at both the transmitter and receiver. It supports spatial multiplexing, allowing several data streams to be transmitted simultaneously over the same frequency band. MIMO significantly boosts data rates and spectral efficiency and is a key technology in 4G LTE and Wi-Fi [7].

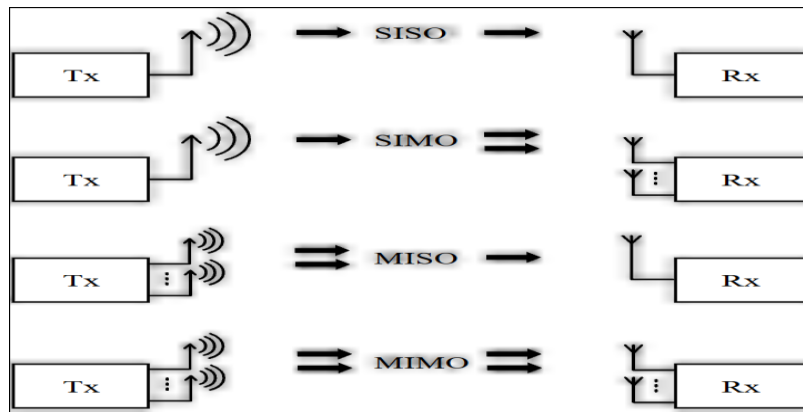


Figure I 5: Illustration of SISO, SIMO, MISO, MIMO [8]

I.4.2.5 Massive MIMO is an extension of MIMO that uses dozens or even hundreds of antennas, especially at the base station. It enables simultaneous communication with many users by forming focused beams. This dramatically increases capacity and efficiency, making it essential for 5G. However, it also introduces challenges like pilot contamination and high computational requirements [7].

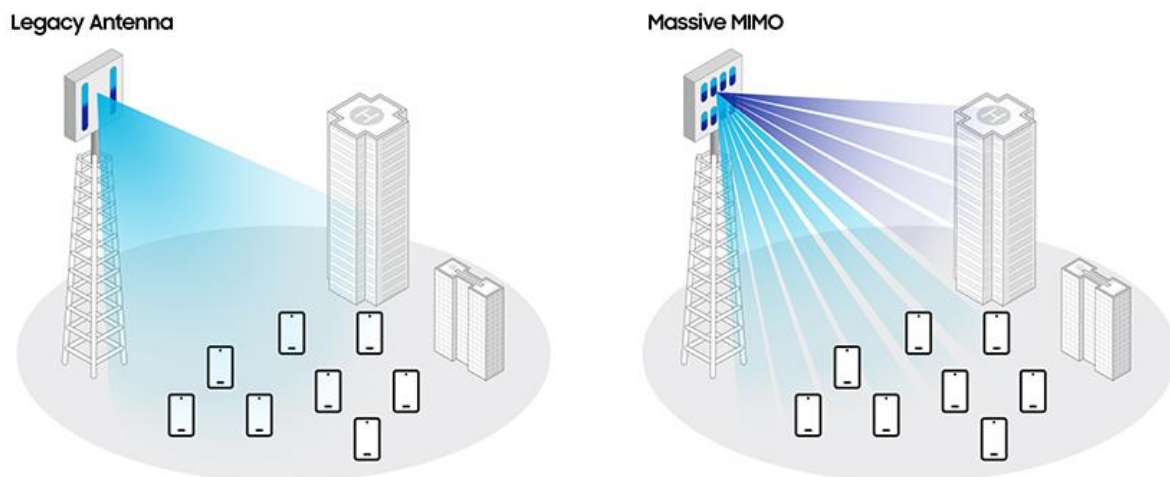


Figure I 6: Coverage comparison between legacy antenna and Massive MIMO [9]

I.4.3 Millimeter Waves: In-Depth Theoretical Overview

Millimeter-wave (mmWave) communications, operating in the 30–300 GHz spectrum, represent a foundational shift in the physical layer design of 5G networks. Within this band, specific ranges such as 28 GHz, 38 GHz, 60 GHz, and the E-band (71–76 GHz and 81–86 GHz) are especially important for practical deployment. These frequencies offer extremely wide bandwidth—on the order of gigahertz—allowing for multi-gigabit data rates, which are crucial for ultra-high-definition video, real-time applications, and dense user environments.

However, these benefits come with severe propagation challenges. Due to their short wavelength, mmWave signals suffer from high free-space path loss, molecular absorption (notably by oxygen around 60 GHz), and significant rain attenuation. For example, atmospheric absorption at 60 GHz can reach 15–30 dB/km, while heavy rain can cause attenuation exceeding 2 dB over just 200 meters. Consequently, mmWave coverage is typically limited to ~200 meters, making it more suited to small-cell architectures [10].

Additionally, mmWave signals are highly directional and sensitive to blockage. Simple obstructions—such as a human body or tree—can degrade the signal by 20–30 dB. The weak diffraction capability also means mmWave cannot easily "bend" around obstacles. This necessitates precise beamforming and beam alignment, achieved through electronically steerable phased-array antennas.

Here, multiple antenna systems such as MIMO and Massive MIMO have become essential. By deploying large antenna arrays, mmWave systems can use spatial multiplexing to send multiple streams in parallel, increasing data throughput. Moreover, Massive MIMO at mmWave frequencies enhances beamforming precision and mitigates path loss by focusing energy in narrow beams. Yet, these systems face practical limits: traditional baseband precoding used in sub-6 GHz MIMO does not scale efficiently at mmWave due to hardware constraints and fewer multipath components. This has led to hybrid analog/digital beamforming architecture tailored for mmWave transceivers [10].

The characteristics of mmWave propagation directly influence system-level design, including small-cell placement, antenna configurations, and protocol architectures. Advanced solutions like relay nodes, multi-AP diversity, and multi-hop MAC protocols are being developed to combat frequent link outages and mobility-induced dynamics.

In conclusion, while mmWave communication unlocks extraordinary capabilities in terms of capacity and speed, its deployment depends heavily on integrating it with multiple antenna systems like Massive MIMO, which compensate for its limitations through spatial gain and flexibility.

I.4.4 Network slicing

5G network slicing revolutionizes network architecture by enabling multiple independent virtual networks to operate simultaneously on a shared physical infrastructure. This transformative capability represents one of 5G's most significant advancements, as it

allows a single network to simultaneously accommodate diverse services with radically different requirements - from ultra-low latency communications for autonomous vehicles to high-reliability connections for critical voice services - all while maintaining strict performance isolation between slices.[10]

The use cases identified for 5G and network slicing fall into three major categories:

1.4.4.1 Enhanced mobile broadband (eMBB): Designed to meet the growing demand for high-speed connectivity, eMBB offers peak data rates of up to 20 Gbps—nearly ten times faster than 4G. Leveraging millimeter-wave (mmWave) frequencies (24–100 GHz) and advanced modulation techniques like 256QAM, it enables seamless 8K video streaming and immersive virtual and augmented reality experiences.

1.4.4.2 Ultra-Reliable low-latency communications (URLLC): Tailored for mission-critical applications, URLLC delivers end-to-end latency as low as 1 millisecond, with reliability reaching 99.9999%. This level of performance is essential for technologies like autonomous vehicles, remote medical procedures, and industrial automation, where split-second responsiveness can be crucial.

1.4.4.3 Massive machine-type communications (mMTC): Supporting up to one million connected devices per square kilometer, mMTC empowers large-scale IoT deployments, from smart city infrastructure and intelligent transportation systems to smart factories and precision agriculture. This is enabled through technologies like NB-IoT and grant-free uplink transmission.[10]

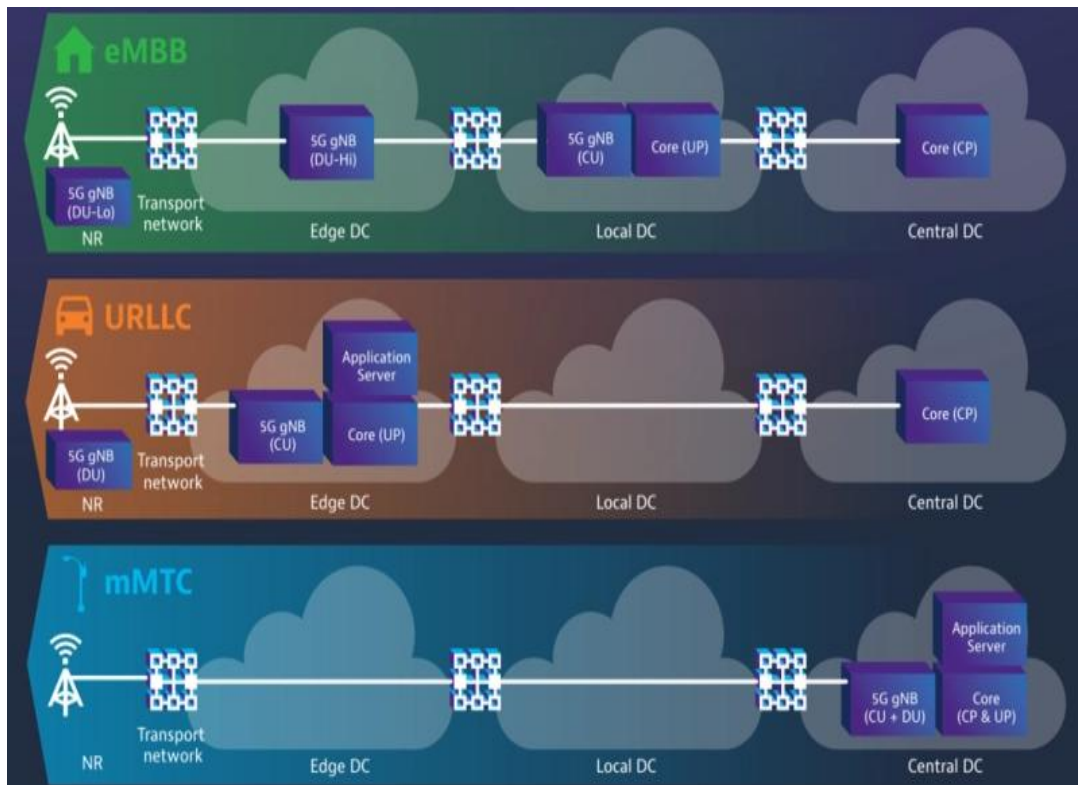


Figure I 7: 5G Network Slicing Categories: eMBB, URLLC, and mMTC. [11]

I.4.5 Edge computing

Multi-access Edge Computing (MEC) decentralizes data processing by deploying micro-data centers at 5G base stations, reducing latency to <10ms for time-sensitive applications. This paradigm supports local AI processing for autonomous systems and bandwidth conservation through edge filtering (e.g., selective video analytics at smart cameras). The European Telecommunications Standards Institute (ETSI) MEC standards (2023) highlight its role in enabling real-time industrial automation and privacy-preserving applications. However, large-scale deployment faces challenges in infrastructure costs and vendor interoperability.[10]

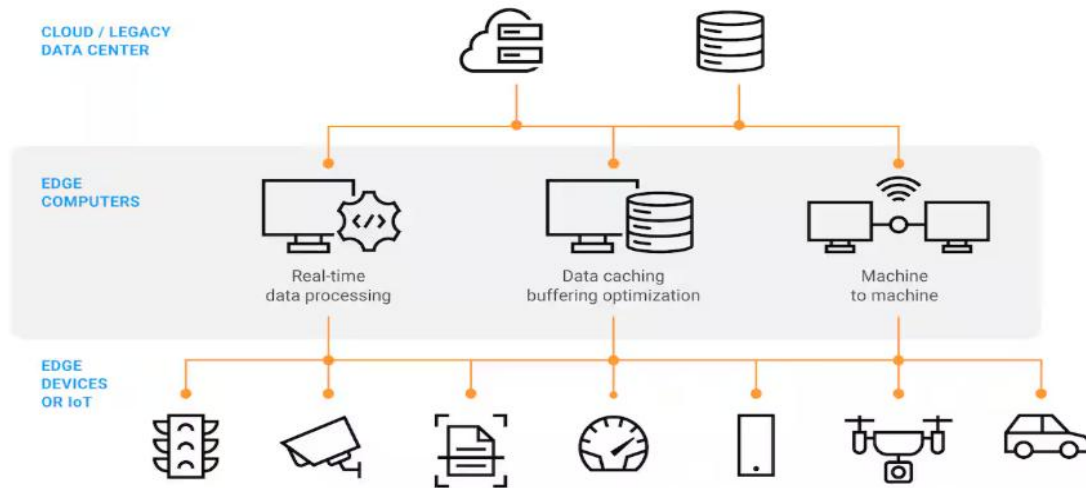


Figure I 8: Edge computing role in the 5g network [12]

I.5 Challenges of 5G

Accurate modeling of wireless channels is essential for the successful design and evaluation of 5G systems. Unlike previous generations, 5G operates across a much wider range of frequencies, including the challenging millimeter-wave (mmWave) bands, where signal behavior becomes highly sensitive to environmental factors such as obstructions, reflections, and mobility. These characteristics introduce new complexities in how signals propagate, especially in urban and indoor environments where multipath components and blockages are frequent. Conventional channel models that assume static or independent behavior across space fall short of capturing the dynamic nature of 5G deployments. [13]

I.6 Conclusion

As a result, one of these challenges in 5G lies in representing how channel characteristics evolve as users move. This leads to the concept of spatial consistency, which ensures that parameters such as delay spread, angle of arrival, and power change gradually and realistically over space and time. Incorporating spatial consistency into 5G channel models is crucial for evaluating technologies like beamforming, mobility management, and real-time handover in a way that reflects true network behavior.

Chapter II: The spatial consistency parameters of the channel

Chapter II

The spatial consistency parameters of the channel

II.1 Introduction

The study of wireless channel modeling for millimeter wave (mmWave) frequencies has gained significant importance in 5G network development, with extensive research conducted across various environmental scenarios. A critical challenge in mmWave channel characterization involves maintaining spatial consistency in statistical propagation analysis. This property ensures that as a user moves along a trajectory, the channel impulse response demonstrates correlation and continuity across successive sampling points. Fundamentally, spatial consistency describes the preservation of similar scattering characteristics across both large-scale and small-scale propagation environments. For practical modeling purposes, channel scenarios are typically categorized into indoor/outdoor environments, with outdoor conditions further classified as urban microcell (UMi), urban macrocell (UMa), and rural macrocell (RMa) configurations, each considering both line-of-sight (LOS) and non-line-of-sight (NLOS) propagation conditions.

Modern statistical channel models incorporate comprehensive parameters including shadow fading (SF), propagation delay, time clusters, and angular spreads. These large-scale characteristics are fundamentally determined by small-scale parameters such as excess delay, received power levels, angle of arrival (AoA), and angle of departure (AoD) for individual multipath components. This chapter presents the theoretical fundamentals of this whole study.

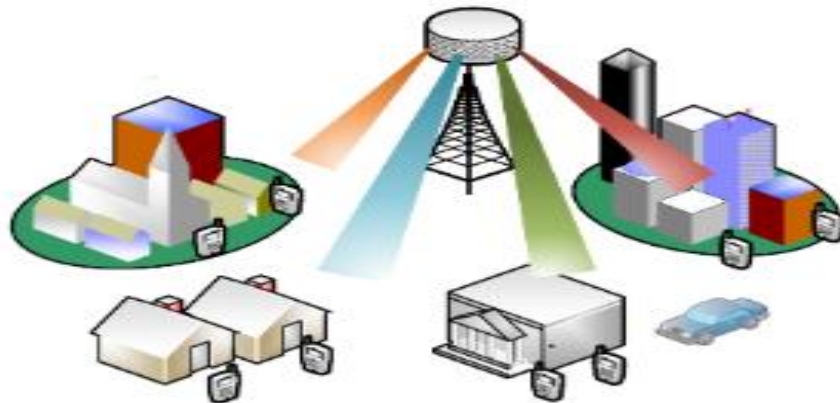


Figure II.1: 5G Base Station Serving Multiple Urban and Suburban Environments. [14]

II.2 Definition of spatial consistency

Spatial consistency refers to the requirement that a wireless channel model produces channel parameters that vary smoothly and correlated over space, so that a mobile user (or closely-located users) experiences a similar scattering environment as they move or as their locations change slightly. In other words, as a user moves along a trajectory, the successive channel impulse responses remain correlated rather than jumping abruptly. This ensures that large-scale and small-scale channel parameters (path loss, shadowing, delays, angles, etc.) change gradually over distance. For example, under spatial consistency when the user moves along a given track the channel impulse response produces a correlated and sequential channel impulse response at successive sample points on the track. Similarly, describing spatial consistency as the phenomenon that a moving user (or multiple nearby users) experiences a similar scattering environment in a local area (e.g., within 15 m), indicating the channels across these locations are spatially correlated. [15]

II.3 Channel parameters affecting spatial consistency

To understand how spatial consistency manifests in real-world wireless environments, it is essential to examine the key channel parameters that govern its behavior. In what follows, we detail the main characteristics starting with path loss that significantly influence the degree of spatial correlation in 5G communication systems.

II.3.1 Path Loss

Path loss is the large-scale attenuation of a transmitted signal as it propagates through space. It is typically expressed in decibels (dB) as the difference between the transmitted and received power (ignoring antenna gains). In mmWave channel models like NYUSIM, path loss is modeled by the close-in (CI) free-space reference model:

$$PL_{cl}(f, d)[dB] = FSPL(f, 1m)[dB] + 10n\log(d) + AT[dB] + X_{\sigma} \quad (\text{II } 1)$$

Where d is the TX–RX separation (m), n is the path loss exponent (e.g. 2 in free space), AT is an atmospheric absorption term, and X_{σ} is a zero-mean log-normal shadow fading term, The free-space path loss at 1 m and frequency f (GHz) is:

$$FSPL(f, 1m)[dB] = 20\log\left(\frac{4\pi f \times 10^9}{c}\right) = 32.4 + 20\log(f)(dB) \quad (\text{II } 2)$$

With spatial consistency, path loss varies smoothly as a user moves, because correlated shadowing (SF) is used instead of independent samples. With spatially correlated SF, the path loss along a 40 m trajectory changes gradually, whereas independent SF produces erratic ~16 dB jumps. Typically, large-scale correlation distances are on the order of 10–15 m in urban microcell scenarios, meaning shadow fading (and hence path loss) remains highly correlated within that range.[15]



Figure II.2: Showcase of path loss [16]

II.3.2 Received Signal Power

The received signal power P_{rx} is the power captured at the receiver antenna from the transmitted signal. In practice it is computed by a link-budget:

$$P_{rx} = P_{tx} + G_t + G_r - PL \quad (II\ 3)$$

Where P_{tx} is transmitted power and G_t , G_r are TX/TR antenna gains. In the omnidirectional (isotropic) sense, NYUSIM also computes the total received power by summing all multipath component (MPC) powers from the Power delay profile.

Because P_{rx} directly depends on path loss and shadow fading, spatial correlation in those large-scale effects yields smooth changes in received power as the user moves. For example, even with directional antennas, the averaged received power remains highly correlated for motions up to ~5 m in urban microcell settings. In practice, this means a user moving a few meters will see only gradual power fluctuations (aside from blockages) rather than random jumps. Spatially consistent modeling in NYUSIM ensures that as shadow fading is correlated over ~10–15 m, the received power similarly evolves smoothly along the track. [15]

II.3.3 Power Delay Profile (PDP)

The power delay profile (PDP) describes how received signal power is distributed over time delays due to multipath. Formally, for a multipath channel with L paths of complex amplitude a_ℓ and delay τ_ℓ , the instantaneous PDP can be written as:

$$P(\tau) = \sum_{\ell=1}^L |a_\ell|^2 \delta(\tau - \tau_\ell) \quad (\text{II } 4)$$

Equivalently, the average PDP is $E[|h(t,\tau)|^2]$, where $h(t,\tau)$ is the channel impulse response. In NYUSIM, the PDP is organized into time clusters (groups of MPCs close in delay) and spatial lobes (groups close in angle), though the PDP itself sums over all arrival directions to give total power vs. delay.

The PDP (and its derived metrics like mean and RMS delay spread) also varies with user position and must exhibit spatial correlation. Measurements in an urban street canyon showed that large-scale PDP statistics have short correlation distances – on the order of 5–10 m. For example, the number of time clusters and the delay spread each stayed correlated over roughly 5–10 m of movement. Moreover, transitions between LOS and NLOS cause abrupt changes: at one NLOS point the measured PDP had only 1 cluster, whereas just a few meters away in LOS it jumped to 6 clusters with much higher total power. Spatially consistent models in NYUSIM account for this by tracking clusters (birth/death) and LOS state along the route, rather than re-generating an independent PDP at each point. In short, as the user moves, the PDP evolves smoothly (clusters persist or fade gradually) so that delays and powers are correlated across nearby locations. [16]

II.3.4 Shadow Fading

Shadow Fading (SF), also called large-scale fading, represents the signal strength variations caused by obstructions like buildings, trees, or terrain that block the signal over distances ranging from several meters to hundreds of meters as illustrated in figure II.3.

It is usually modeled as a log-normal distribution:

$$SF_{dB} \sim N(0, \sigma^2) \quad (\text{II } 5)$$

Where:

σ is the standard deviation in dB, typically ranging from 4 to 12 dB depending on the environment.

N is the symbol for a normal distribution, also known as a Gaussian distribution.

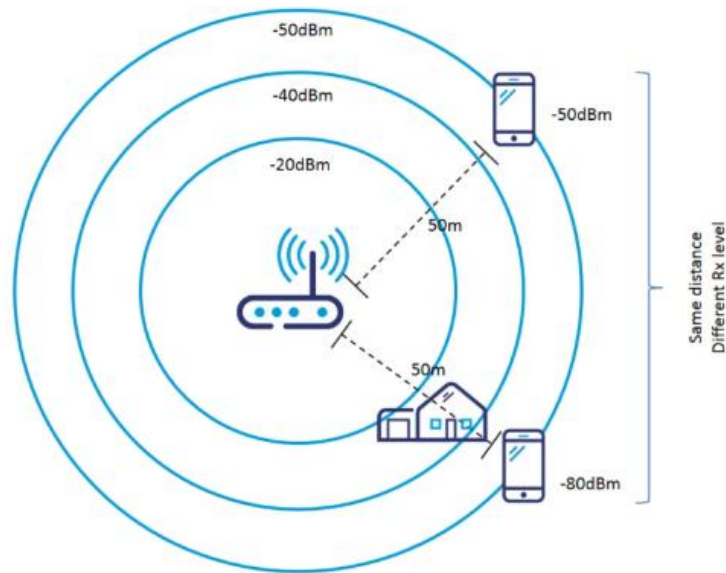


Figure II.3: Shadow fading impact. [18]

In a spatially consistent model, SF values change smoothly across space, meaning nearby users experience correlated shadowing. If SF is modeled independent, it causes abrupt unrealistic variations, breaking spatial correlation. [16]

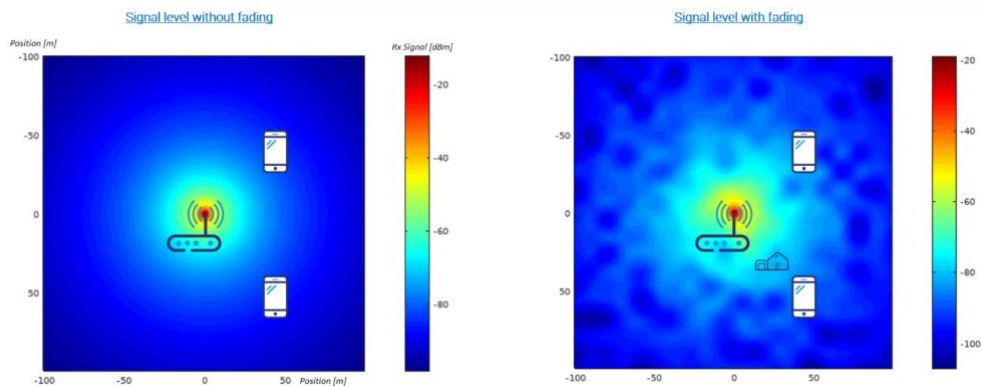


Figure II.4: Difference in signals with and without shadow fading. [19]

II.3.5 Angle of Arrival (AoA)

AoA is the direction (azimuth and elevation) from which each Multipath Component (MPC) reaches the receiver.

It's often modeled with a mean angle and angular spread (AS), e.g.:

$$AoA_i \sim N(\mu_\theta, \sigma_\theta^2) \quad (\text{II } 6)$$

Where:

μ_θ = mean AoA

σ_θ = angular spread

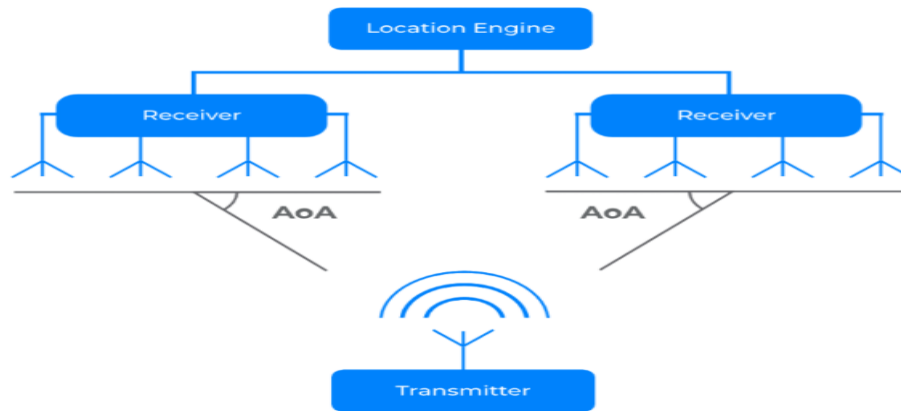


Figure II 5: Angle of arrival demonstration [20]

The Angle of Arrival (AoA) significantly influences spatial consistency in wireless channels. In practical terms, AoA determines the direction from which multipath components reach the receiver. This parameter is critical for advanced techniques like beamforming and accurate user tracking. When spatial consistency is well-preserved, the AoA changes smoothly as a user moves through space, ensuring a stable and realistic propagation environment. However, if there are abrupt or uncorrelated shifts in AoA between nearby spatial points, it indicates a lack of spatial coherence in the channel model. Such inconsistencies can degrade the performance of directional antennas and tracking algorithms. Therefore, maintaining gradual transitions in AoA is essential for simulating realistic and spatially consistent 5G propagation channels.[21]

II.3.6 Angle of Departure (AoD)

AoD is the direction (azimuth and elevation) at which a signal leaves the transmitter on its way to the receiver. Like AoA, it's modeled using angular statistics.

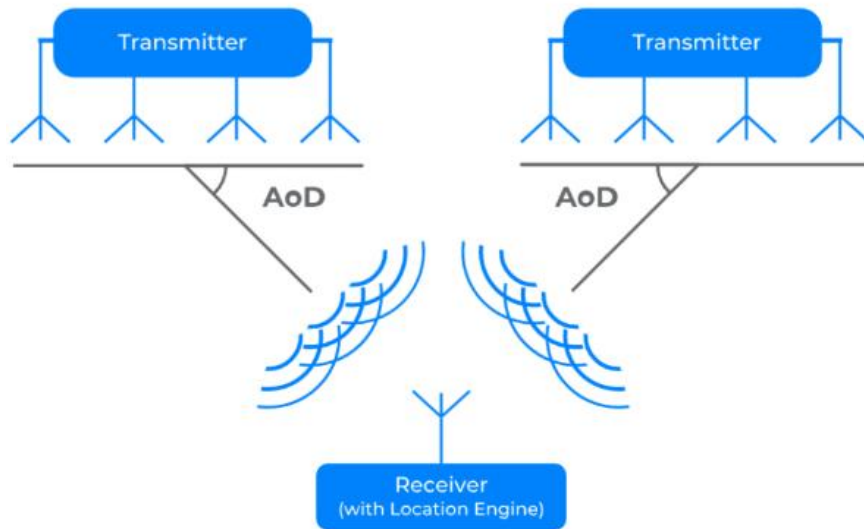


Figure II 6: Angle of departure demonstration[20]

The Angle of Departure (AoD) represents the direction in which multipath components are transmitted from the base station or transmitter toward the receiver. It plays a critical role in beamforming strategies and the overall directionality of signal propagation. In spatially consistent channel models, AoD values should vary smoothly with user movement to reflect realistic propagation conditions. When AoD exhibits spatial coherence, it enables accurate modeling of beam steering and transition between beams in multi-antenna systems. On the other hand, abrupt or uncorrelated changes in AoD between nearby locations can lead to unrealistic beam misalignments, negatively impacting the performance of directional transmissions. Therefore, preserving gradual and continuous variations in AoD is essential for reliable simulation and analysis of 5G systems, particularly in scenarios involving user mobility and dynamic beam management. [22]

II.4 Importance of Spatial Consistency in 5G Applications

Spatial consistency plays a crucial role in the realistic modeling and simulation of 5G wireless communication systems. Unlike earlier stochastic models, where channel parameters were often generated independently at each location, spatial consistency ensures that the wireless channel varies smoothly as a function of position. This means that as a mobile user moves, the evolution of key channel characteristics such as path loss, delay spread, shadowing, and angular information remains continuous and spatially correlated. This continuity is critical for accurately predicting and optimizing performance in a wide range of real-world applications.

II.4.1 Mobility and Handover Management

In mobile environments, users frequently transition from one base station’s coverage area to another. Effective handover mechanisms depend on the ability to predict how the channel will evolve along a user’s trajectory. Spatial consistency enables accurate modeling of signal strength, delay spread, and interference across space, allowing mobility management algorithms to anticipate link degradation and proactively trigger handovers as we can see in figure II 7 and figure II 8. Without spatial correlation, simulations might produce erratic or unrealistic transitions, leading to poor handover decisions and degraded Quality of Service (QoS) in practice.

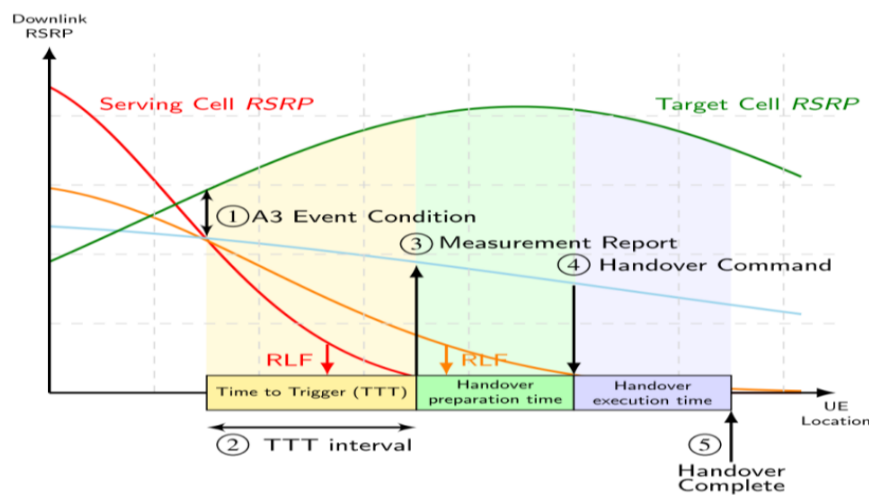


Figure II 7: Typical 5G handover graph showing signal strength from source and target cells over distance/time [23]

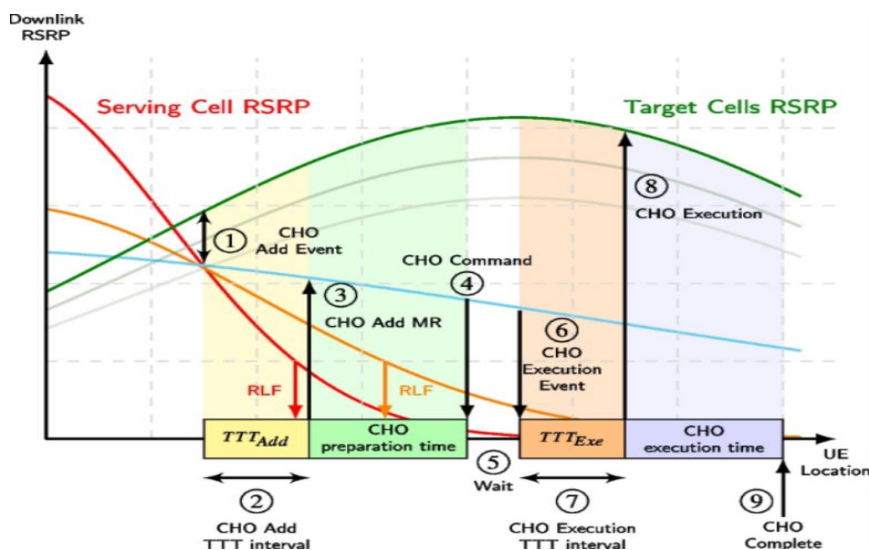


Figure II 8: Beam outage probability vs wind speed [23]

II.4.2 Beamforming and Beam Tracking

Beamforming is a fundamental technology in 5G, especially in millimeter-wave (mmWave) systems where narrow beams are used to overcome high path loss. For beamforming and beam-tracking algorithms to perform well, it is essential that the direction-of-arrival (AoA) and direction-of-departure (AoD) of multipath components vary smoothly as the user moves. Spatial consistency ensures these angular parameters remain continuous, which allows for stable and reliable beam alignment. In contrast, sudden angular shifts due to inconsistent channel modeling can cause beam misalignment, loss of connectivity, and reduced throughput, figure II.9 explains it more.

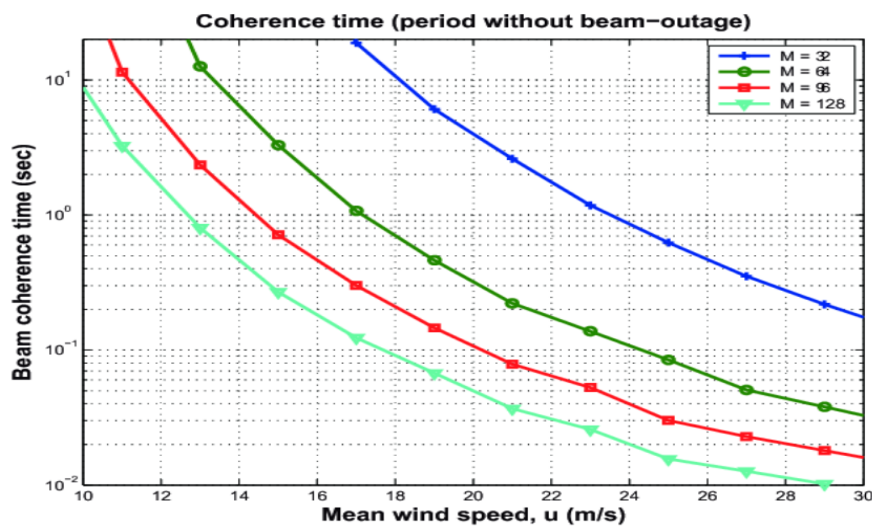


Figure II 9: Graph of spatial correlation function (SCF) versus antenna spacing in vehicular MIMO contexts [24]

II.4.3 Massive MIMO Channel Estimation

Massive Multiple Input Multiple Output (MIMO) systems leverage spatial diversity by using a large number of antennas. Spatial consistency ensures that the channel estimates across antenna elements and over space are realistic and correlated. This is important for accurate channel state information (CSI) acquisition, which directly affects precoding, beam selection, and user grouping in multi-user scenarios. Inconsistent models can introduce noise into channel estimates, reducing spectral efficiency and system reliability.

II.4.4 Augmented/Virtual Reality and Latency-Sensitive Applications

Emerging applications such as augmented reality (AR), virtual reality (VR), and tactile internet services require ultra-reliable low-latency communication (URLLC). These

applications often involve users moving within confined spaces (e.g., rooms, streets, or vehicles), and any abrupt variations in the channel can lead to noticeable disruptions. Spatially consistent modeling provides smooth transitions in channel characteristics, ensuring stable connections, predictable latency, and high user quality-of-experience (QoE). For instance, a VR user moving their head rapidly within a few meters should not experience erratic network behavior due to an unrealistic channel model.

II.4.5 Vehicular Communication Systems

In vehicle-to-everything (V2X) communication scenarios, high-speed mobility and rapidly changing environments make spatial consistency even more critical. A car moving along a road must maintain a reliable connection with roadside units or other vehicles, and sudden changes in channel behavior can lead to signal drops, increased delay, or loss of safety-critical information. Spatially consistent models allow for more accurate emulation of these dynamic conditions, supporting the development of robust vehicular communication protocols and safety applications. [25]

II.5 Conclusion

In this chapter, we have explored the theoretical foundation necessary to understand spatial consistency in the context of 5G wireless communication systems. Spatial consistency, which ensures that channel characteristics evolve smoothly as a user moves through space, is essential for accurately modeling dynamic wireless environments and enabling realistic simulations in tools such as NYUSIM. A detailed analysis of key parameters—namely, Path Loss, Received Signal Power, and Power Delay Profile—has revealed how each metric contributes to or reflects the level of spatial coherence in a propagation scenario. Additional factors such as Shadow Fading, Angle of Arrival (AoA), and Angle of Departure (AoD) further influence spatial consistency by affecting how multipath components behave over space. Together, these parameters determine the fidelity and realism of channel models used in 5G research and development. Understanding and accurately simulating their behavior not only enhances system performance analysis but also supports the design of robust and efficient communication systems. This theoretical foundation sets the stage for the practical investigation of spatial consistency effects using simulation tools, which will be presented in the following chapter.

Chapter 3: Simulation and results

Chapter III

Simulation and results

III.1 Introduction

This chapter presents a simulation-based evaluation of how spatial consistency impacts 5G wireless communication channels. The analysis is conducted using NYUSIM, a channel simulator developed by NYU WIRELESS that supports modeling of millimeter-wave (mmWave) propagation in urban environments. By enabling spatial consistency, NYUSIM allows us to observe how key channel metrics evolve with user mobility.

Our goal is to assess the effect of spatially correlated parameters such as shadow fading correlation distance, LOS/NLOS transition smoothing, and update resolution on propagation characteristics like path loss, received power, delay spread, and angular dispersion. Simulations are carried out for typical Urban Microcell (UMi) conditions at 28 GHz, with parameter values chosen to reflect realistic mobility scenarios and environmental conditions in a hot, semi-arid region.

III.1.1 Legacy programs and tools

Before the introduction of NYUSIM, most legacy channel simulators generated independent channel realizations at each user position and did not support spatial consistency, resulting in unrealistic channel variations during user mobility. NYUSIM was therefore chosen in this work because it provides a measurement-based spatial consistency framework that ensures smooth and physically realistic evolution of channel parameters along user trajectories, which is essential for accurate 5G mmWave mobility analysis.

To better highlight the advantages of NYUSIM, the following subsection briefly reviews the main legacy channel simulation tools that were commonly used prior to the adoption of spatially consistent models.

III.1.1.1 3GPP SCM MATLAB Channel Simulator

The 3GPP SCM MATLAB simulator was one of the earliest tools used to generate wireless channel realizations for cellular systems. It models multipath propagation and MIMO effects using statistical assumptions defined by 3GPP. This simulator was mainly used for early studies on antenna diversity and MIMO performance in sub-6 GHz cellular networks, but it

generates independent channel snapshots and does not account for realistic channel evolution during user movement.

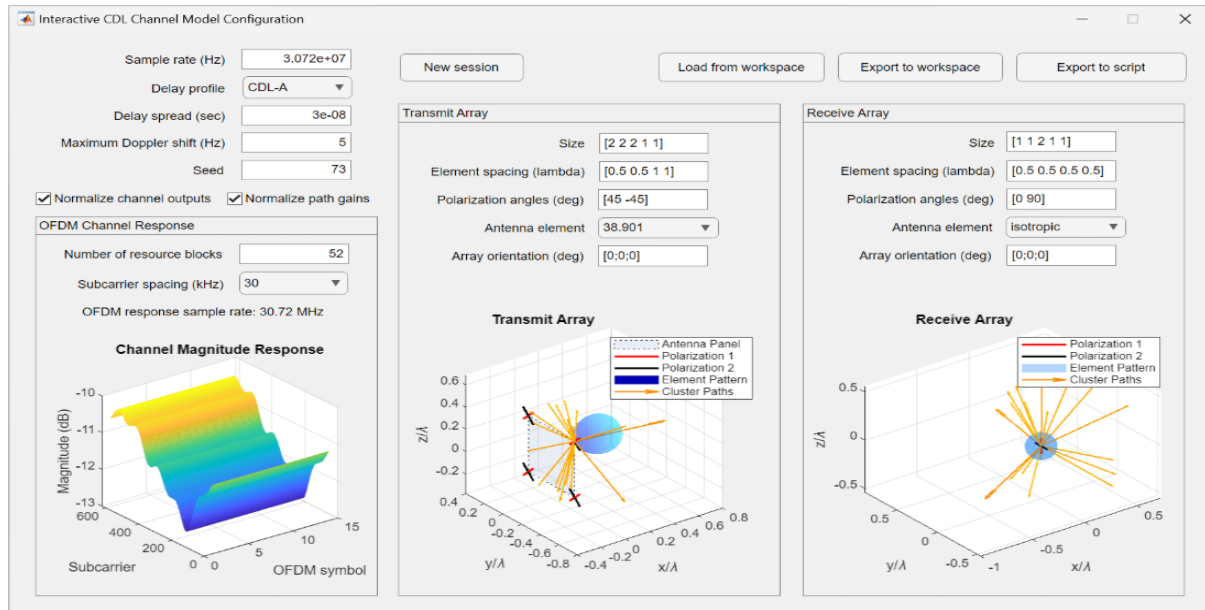


Figure III.1: GUI of 3GPP SCM.[32]

III.1.1.2 WINNER II Channel Simulator

The WINNER II channel simulator was developed to improve the realism of wireless channel simulations compared to SCM. It supports several indoor and outdoor scenarios and provides clustered multipath channel responses for MIMO systems. Although it offers more flexibility and better parameter modeling for LTE and pre-5G studies, channel realizations are still largely independent in space, which limits its ability to accurately represent user mobility.

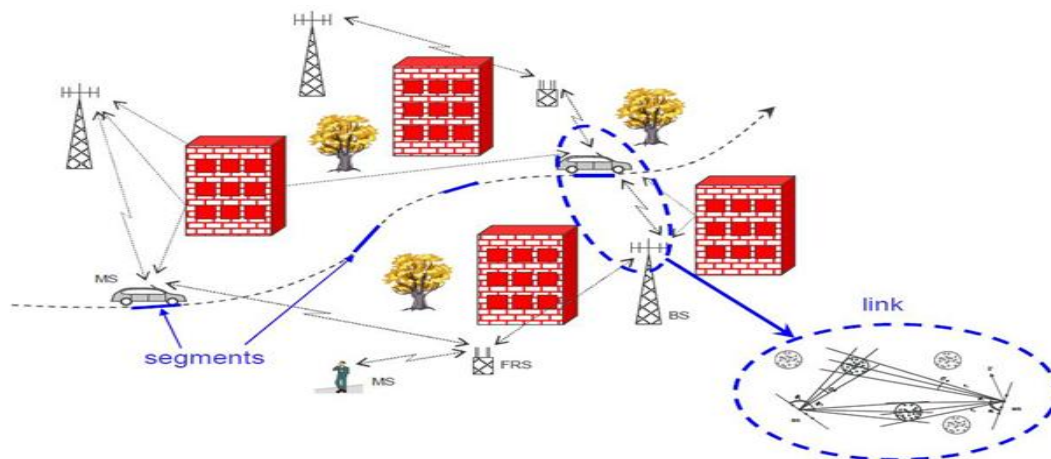


Figure III.2: GUI of WINNER II.[33]

III.1.1.3 COST 2100 Channel Simulator

The COST 2100 channel simulator introduced a more advanced approach by modeling the wireless channel using clusters and visibility regions. This allowed channel characteristics to evolve gradually as the user moves, making it one of the first tools to partially address spatial correlation. However, it was mainly designed for sub-6 GHz frequencies and does not fully capture the directional and wideband characteristics of mmWave channels.



Figure III.3: GUI of COST 2100.[34]

III.1.1.4 Wireless InSite (Remcom)

Wireless InSite is a deterministic ray-tracing simulator that models radio propagation based on detailed three-dimensional representations of the environment. As the transmitter or receiver moves, the channel changes naturally according to reflections, diffractions, and blockages, providing spatially consistent behavior. While this approach is highly accurate for specific sites, it requires detailed environment data and high computational effort, making it less suitable for large-scale statistical studies compared to NYUSIM.

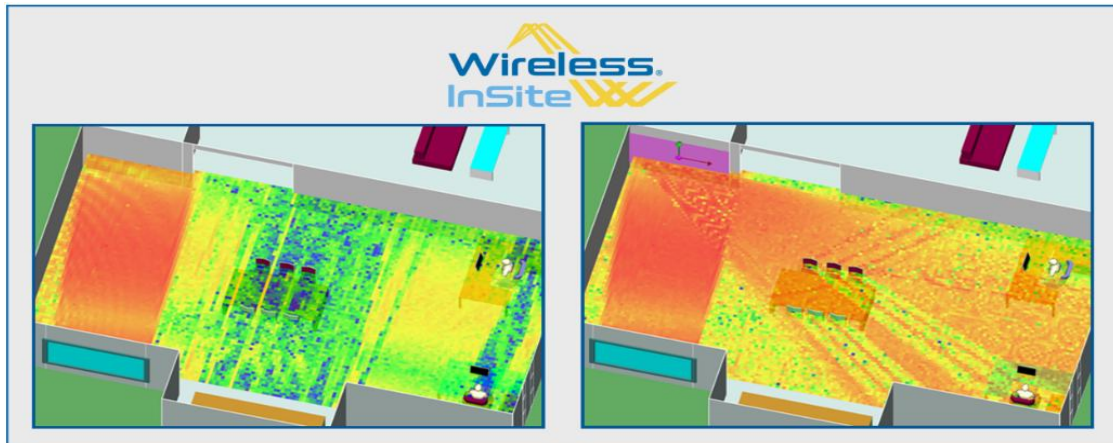


Figure III.4: GUI of Wireless InSite.[35]

III.2 Introduction to NYUSIM

NYUSIM (New York University Simulator) is a MATLAB-based tool developed by NYU WIRELESS (Fig. III.1) to simulate millimeter-wave (mmWave) propagation channels. It provides realistic channel models based on extensive real-world measurements in different environments (Fig. III.2) such as Urban Microcell (UMi), Urban Macrocell (UMa), and Rural Macrocell (RMa).

The simulator enables the configuration of various system parameters such as frequency, bandwidth, antenna configurations, and spatial consistency. It also offers Power Delay Profiles (PDPs), angular spreads, and path loss data that are crucial for analyzing the performance of 5G communication systems.

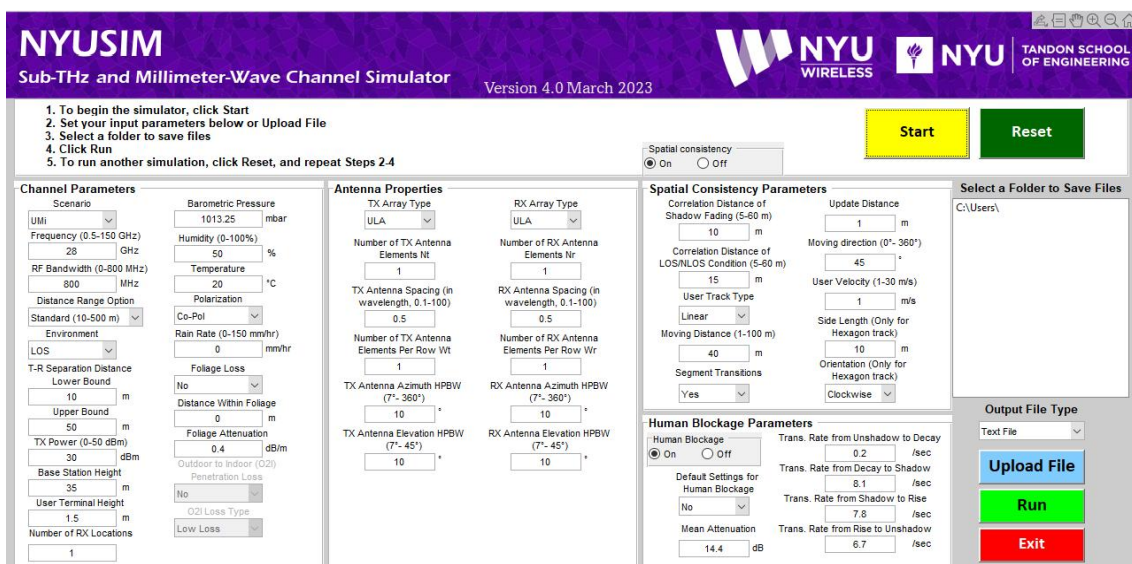


Figure III.5: GUI of NYUSIM.

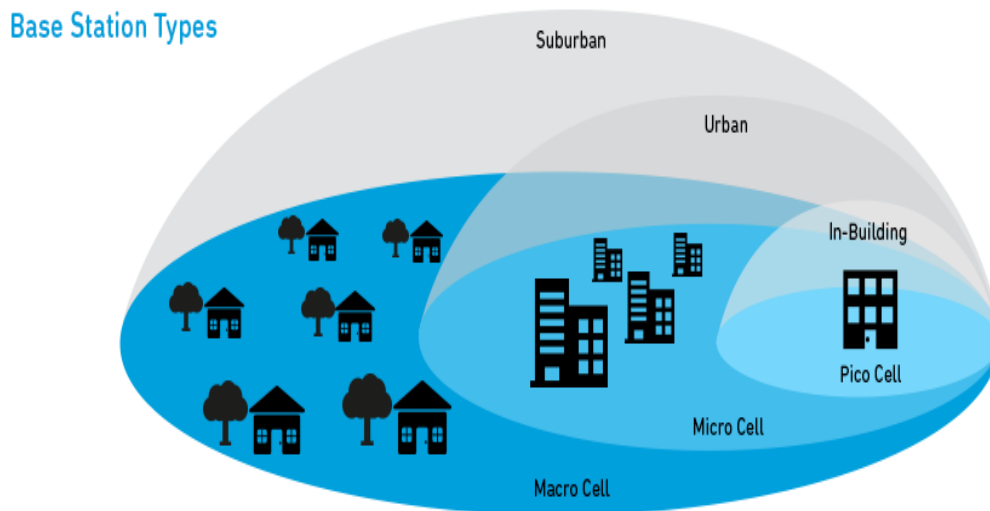


Figure III.6: Types of Base Stations: Pico Cell, Micro Cell, and Macro Cell. [27]

III.3 NYUSIM simulator parameters

In this section, we will describe different NYUSIM simulator parameters such: Channel, Antenna and Spatial consistency parameters.

III.3.1 Channel Parameters

Figure III.7: channel parameters.

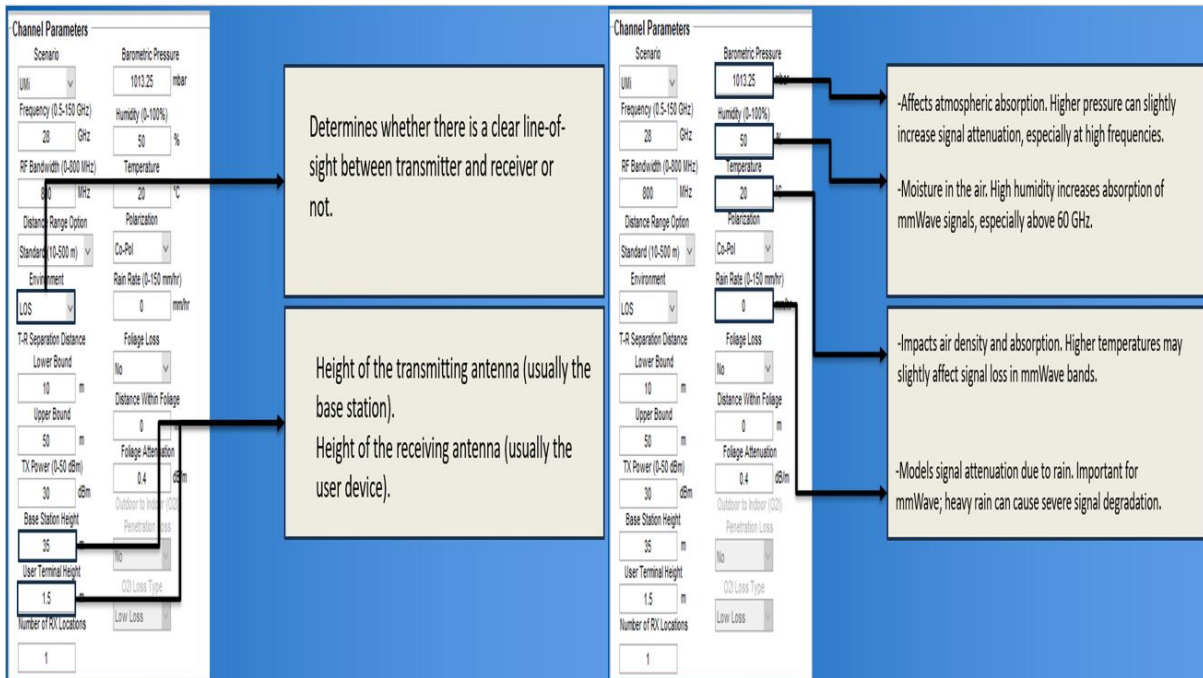


Figure III.8: channel parameters.

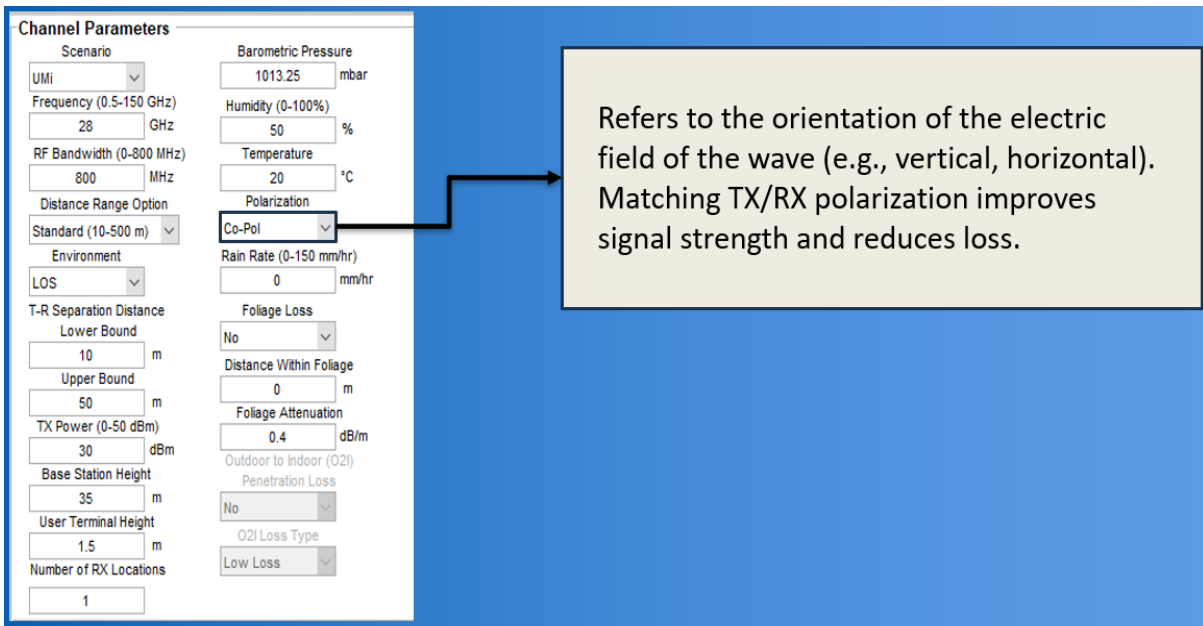


Figure III.9: channel parameters.

Each of these parameters influences the fundamental properties of wireless signal propagation.

● **Scenario:** Urban Microcell (UMI)

Defines the environment for the simulation. UMI represents a dense urban area with low-to-medium building heights, typically used to model mmWave street-level coverage.

● Frequency: 28 GHz

Carrier frequency of the transmitted signal. Higher frequencies like 28 GHz (mmWave band) offer more bandwidth but are more sensitive to path loss and blockages.

● RF Bandwidth: 800 MHz

The width of the frequency band is used for transmission. Larger bandwidth allows higher data rates and finer time resolution in delay profiles.

● Distance Range Option: Standard (10–500 m)

The distance over which the channel is simulated. Standard mode sets lower and upper bounds on TX–RX separation to control path loss and LOS probability.

● Lower Bound / Upper Bound: 100 m / 500 m

Specifies the minimum and maximum distance between the transmitter and receiver during the simulation.

● TX Power: 30 dBm

The power transmitted by the base station, in decibels relative to 1 milliwatt. Affects the received signal strength and SNR.

● Base Station Height: 35 m

The height of the transmitter above the ground, typically on building rooftops in urban environments.

● User Terminal Height: 1.5 m

The height of the receiver, simulating a handheld mobile device at pedestrian level.

● Number of RX Locations: 1

The simulation is conducted for a single RX trajectory rather than multiple spatial points. Useful for controlled mobility analysis.

● Barometric Pressure: 1052.96 mbar

Environmental parameter affecting atmospheric absorption, particularly at mmWave frequencies.

● Humidity: 48.96%

Also contributes to attenuation in the mmWave band due to absorption by water vapor molecules.

- Temperature: 55.31°C

High temperatures slightly increase air density and attenuation, especially at high frequencies.

- Polarization: Co-Polarization

Means the TX and RX antennas use the same polarization (e.g., vertical-vertical), ensuring maximum signal alignment and power transfer.

- Rain Rate: 13.92 mm/hr

Models additional attenuation caused by rain. Higher rain rates increase signal degradation, especially at mmWave.

- Foliage Loss: No

This disables signal attenuation due to trees or vegetation.

- Distance within Foliage: 0 m / Foliage Attenuation: 0.4 dB/m

Even though foliage is disabled, these parameters define how much signal is attenuated if foliage is later activated. 0.4 dB/m is a typical attenuation rate for trees. [27]

III.3.2 Antenna Parameters

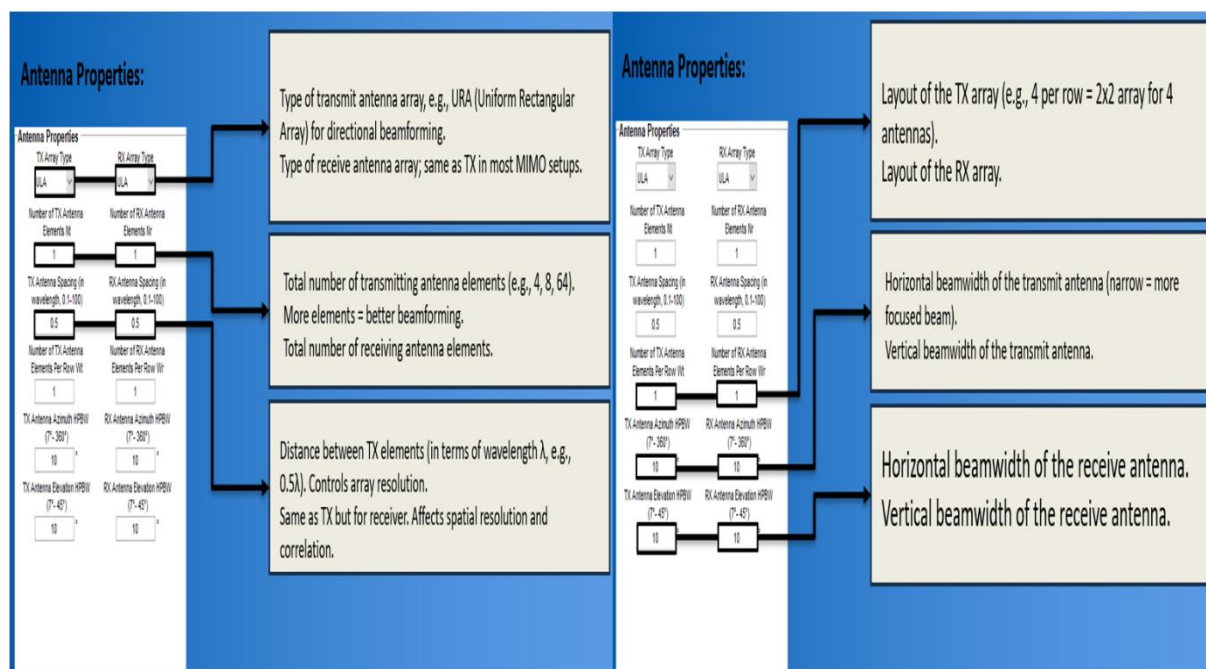


Figure III.10: Antenna parameters.

These define the physical properties and configuration of the antenna arrays.

- TX Array Type: URA (Uniform Rectangular Array)

Antenna elements are arranged in a rectangular grid. Supports beamforming in both azimuth and elevation.

- Number of TX Antennas: 4

Total number of transmitting antenna elements.

- TX Antenna Spacing: 0.5λ

Spacing between antenna elements is half a wavelength, which helps avoid grating lobes and supports accurate beamforming.

- TX Antenna Elements per Row (WT): 4

Defines the layout of the URA; 4 elements per row implies 1 row if total antennas = 4.

- TX Azimuth HPBW: 10° / TX Elevation HPBW: 10°

Half-power beamwidths (HPBW) define how directional the beams are. 10° indicates narrow beams, focusing energy in specific directions.

- RX Array Type: URA

Same as the transmitter, allowing beamforming at the receiver side.

- Number of RX Antennas: 4

Number of receiver antenna elements.

- RX Antenna Spacing: 0.5λ

Same principle as TX spacing; ensures spatial resolution and avoids correlation.

- RX Antenna Elements per Row (WT): 4

Describes the structure of the RX URA array.

- RX Azimuth HPBW: 10° / RX Elevation HPBW: 10°

Narrow beamwidths for angular precision and higher gain, useful for evaluating angle-related spatial consistency.[28]

III.3.3 Spatial Consistency Parameters

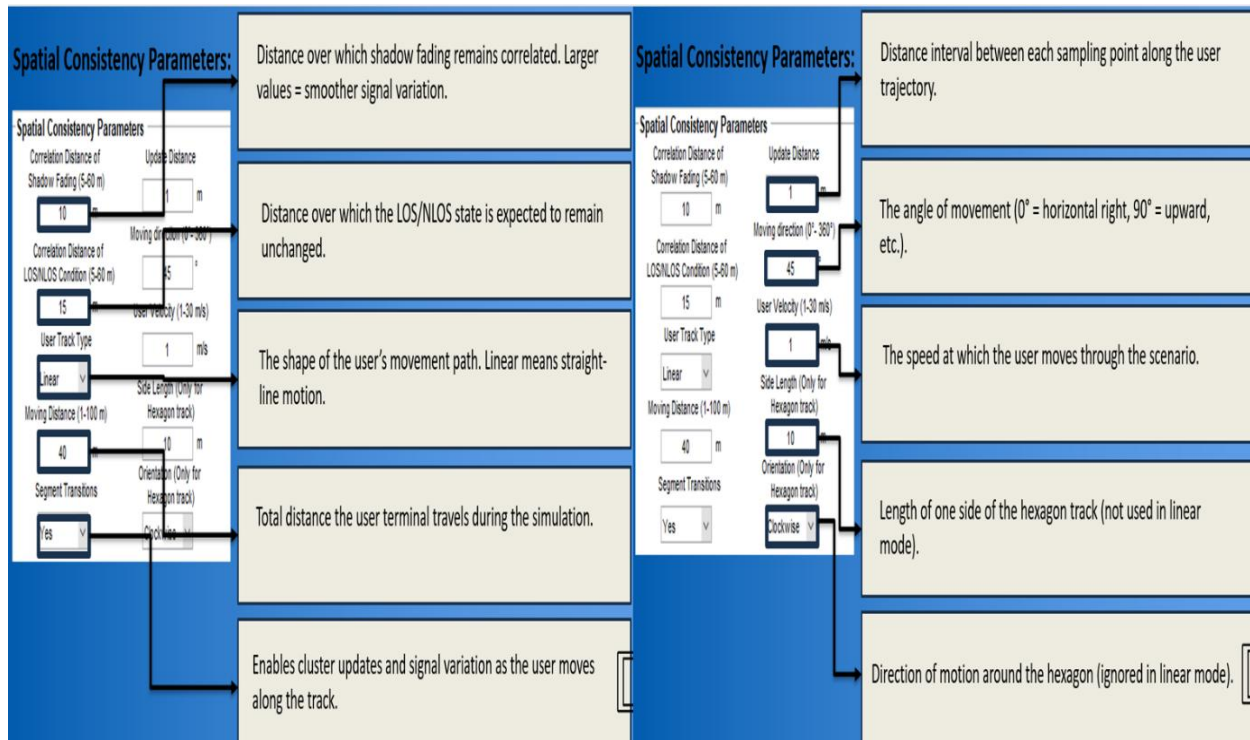


Figure III.11: Spatial consistency parameters.

These parameters control how smoothly the channel evolves as a function of user movement.

- **Correlation Distance of Shadow Fading (SF):** 10 m

Specify the distance over which shadow fading remains correlated. A 10 m setting ensures gradual fading changes over space, simulating realistic large-scale signal variation.

- **Correlation Distance of LOS/NLOS Condition:** 15 m

Controls how long a line-of-sight or non-line-of-sight state persists along the user's path. At 15 m, transitions between LOS and NLOS happen gradually, not randomly.

- **User Track Type:** Linear / Hexagon

Defines the path the user follows. Linear tracks simulate straight movement; hexagonal paths simulate turning corners or complex trajectories.

- **Moving Distance:** 40 m

The total length of the user's motion along the selected path.

- Segment Transitions: Yes

Enables dynamic updates to clusters and angles as the user moves. Essential for spatial consistency studies, especially of AoA, AoD, and PDP.

- Update Distance: 1 m

The simulator updates channel parameters every 1 meter of movement, giving high spatial resolution for tracking parameter changes.

- Moving Direction: 45°

The angle of movement from the origin, where 0° is east. 45° represents the northeast direction.

- User Velocity: 1 m/s

The speed of the moving user. 1 m/s corresponds to typical pedestrian motion.

- Side Length (Hexagon): 10 m

If the hexagonal path is selected, each segment has a length of 10 meters.

- Orientation: Clockwise

Defines the rotational direction along the hexagonal path.[29]

III.4 Simulation parameters justification

To ensure realistic simulation conditions, the environmental parameters were selected to reflect typical climatic characteristics of Biskra, Algeria a representative hot and dry urban area. Table III.1 summarizes average weather data observed in Biskra over recent years, which supports the selection of temperature, humidity, pressure, and rain rate values used in NYUSIM.

Table III.1: Typical Climatic Conditions in Biskra, Algeria for the last 10 years

Parameter	Temperature	Humidity	Pressure	Rain Rate	Foliage Density
Average Value (Approx.)	20–45°C	30–50%	1010–1060 mbar	5–15 mm/hr	Sparse
Notes	Peaks over 50°C in summer	Semi-arid climate	Stable throughout the year	Low rainfall, mostly dry	Desert/semi-desert vegetation

III.4.1 Channel Parameters

- ▶ Carrier Frequency: 28 GHz

This mmWave frequency band are widely used in 5G NR deployments for high-speed data transmission in dense urban areas. It is standardized by 3GPP (band n257) and commonly modeled in NYUSIM for UMi scenarios.

- ▶ RF Bandwidth: 800 MHz

A large bandwidth is essential at mmWave frequencies to support high-throughput services. This value aligns with typical 5G allocations and NYUSIM's support range.

- ▶ Scenario: UMi (Urban Microcell)

This scenario is suitable for environments where base stations are placed at moderate heights (street level or rooftop) and propagation is affected by building density and urban obstacles.

- ▶ TX-RX Distance Range: 100 m to 500 m

These values reflect typical urban microcell deployments. The upper bound represents the maximum reliable range for 28 GHz in urban settings before significant signal attenuation occurs.

- ▶ TX Power: 30 dBm

A common power level for mmWave base stations. It offers sufficient signal strength within the defined UMi range while maintaining safe emission limits.

- ▶ Base Station Height (TX): 35 meters

This height reflects installations on light poles or medium-height buildings in urban areas.

- ▶ User Terminal Height (RX): 1.5 meters

Typical height for handheld mobile devices, representing realistic use cases.

- ▶ Propagation Environment: LOS/NLOS Enabled

This setting allows NYUSIM to dynamically simulate the effects of both Line-of-Sight (LOS) and Non-Line-of-Sight (NLOS) conditions, which are critical for evaluating performance in cluttered urban areas.

III.4.2 Antenna Configuration (MIMO)

- ▶ Array Type: URA (Uniform Rectangular Array) for both TX and RX

URA antennas are used for directional beamforming, a key feature in mmWave 5G to overcome high path loss.

- ▶ Number of Antennas: 4×4 (16 elements)

This configuration provides a balance between beamforming gain and system complexity. It's also a common setup in NYUSIM's supported array options.

- ▶ Antenna Spacing: 0.5λ

Half-wavelength spacing minimizes mutual coupling and ensures constructive interference during beamforming.

- ▶ Half Power Beam Width (HPBW): 10° (Azimuth & Elevation)

Narrow beams are essential for directional communication in mmWave bands to maximize gain and reduce interference. This HPBW simulates focused transmission used in practical deployments.

III.4.3 Spatial Consistency Parameters

- ▶ Shadow Fading Correlation Distance: 10 m

Reflects the smooth variation of shadowing effects over distance. This value aligns with measurements at 28 GHz in urban environments as documented in the NYUSIM technical report and relevant 5G.

- ▶ LOS/NLOS Correlation Distance: 15 m

Ensures realistic evolution of the LOS/NLOS status during mobility. A sudden transition would be non-physical; this parameter controls smoother state changes.

- ▶ User Speed: 1 m/s

Represents a walking pedestrian, which is one of the most common mobility profiles considered in urban 5G studies.

- ▶ Update Distance: 1 m

Allows for frequent updates of spatial channel characteristics, which is crucial when studying the impact of spatial consistency on fast-changing environments.

- ▶ User Track Type: Linear/Hexagonal, Orientation 45°, Moving Distance 40 m

This movement model ensures variation in spatial parameters across a realistic user path, helping to evaluate the channel's spatial behavior.

III.5 Simulation and results

In this section we will observe the results for the different scenarios we did, that includes four scenarios; scenario 1: channel condition will be in line of sight, with shadow fading correlation distance of 10 meters, and on a linear track type.

For scenario two, same settings as the previous scenario only with no line of sight on the channel condition.

The third scenario will change the track type into a hexagonal path, in a line of sight channel condition, and a 10 meters SF correlation distance.

In the last scenario it will be same as scenario three just changing the channel condition to no line of sight.

And all the scenarios have been simulated in 28 GHz frequency, and the rest settings are as we fixed before.

III.5.1 Simulation Setup

The simulations model 28 GHz mmWave propagation in urban NLOS conditions using NYUSim, with a transmitter-receiver separation of 144.0 m. Key parameters include a 10 m shadow fading correlation distance ($\sigma_{sF} = 7.0$ dB), 15 m LOS/NLOS transition correlation, and 1 m/s mobility. The directional and omnidirectional power delay profiles were analyzed with 1.0 m spatial sampling resolution over a 40 m track, capturing time-varying multipath effects and beamforming performance in realistic urban scenarios. We will do a comparative approach that isolates how topology (linear vs. hexagonal) and propagation conditions (LOS vs. NLOS) jointly impact beamforming performance and interference patterns in 5G networks.

III.5.2 Scenario one:

Objective:

This scenario tests how a stable LOS (Line-of-Sight) condition behaves along a straight linear path when the shadow fading correlation distance is moderate (10 m). The goal is to observe baseline signal evolution and beamforming performance in ideal urban conditions.

Table III.2: Parameters used for scenario one

parameter	value
frequency	28(GHz)
Channel Condition	LOS
Shadow Fading Correlation Distance	10m
Track Type	Linear

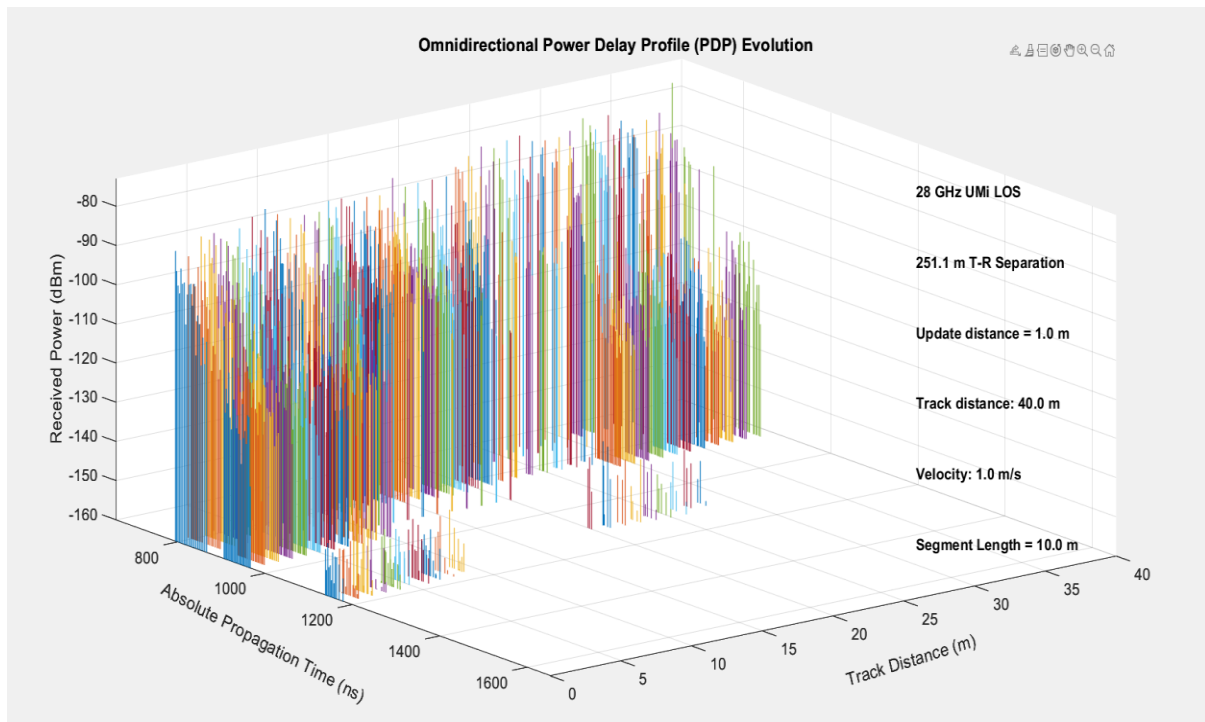


Figure III.12: Omnidirectional PDP for scenario 1

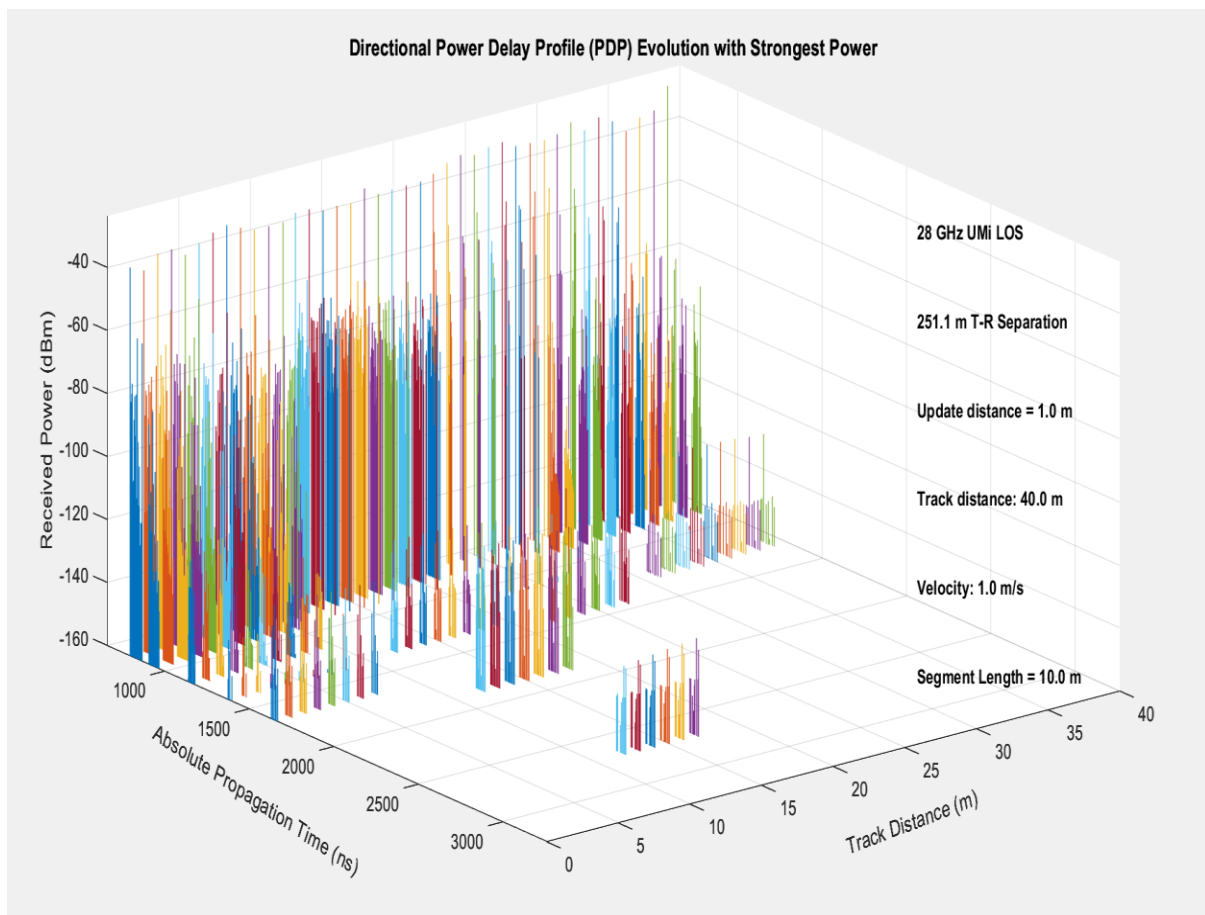


Figure III.13: directional PDP for scenario 1

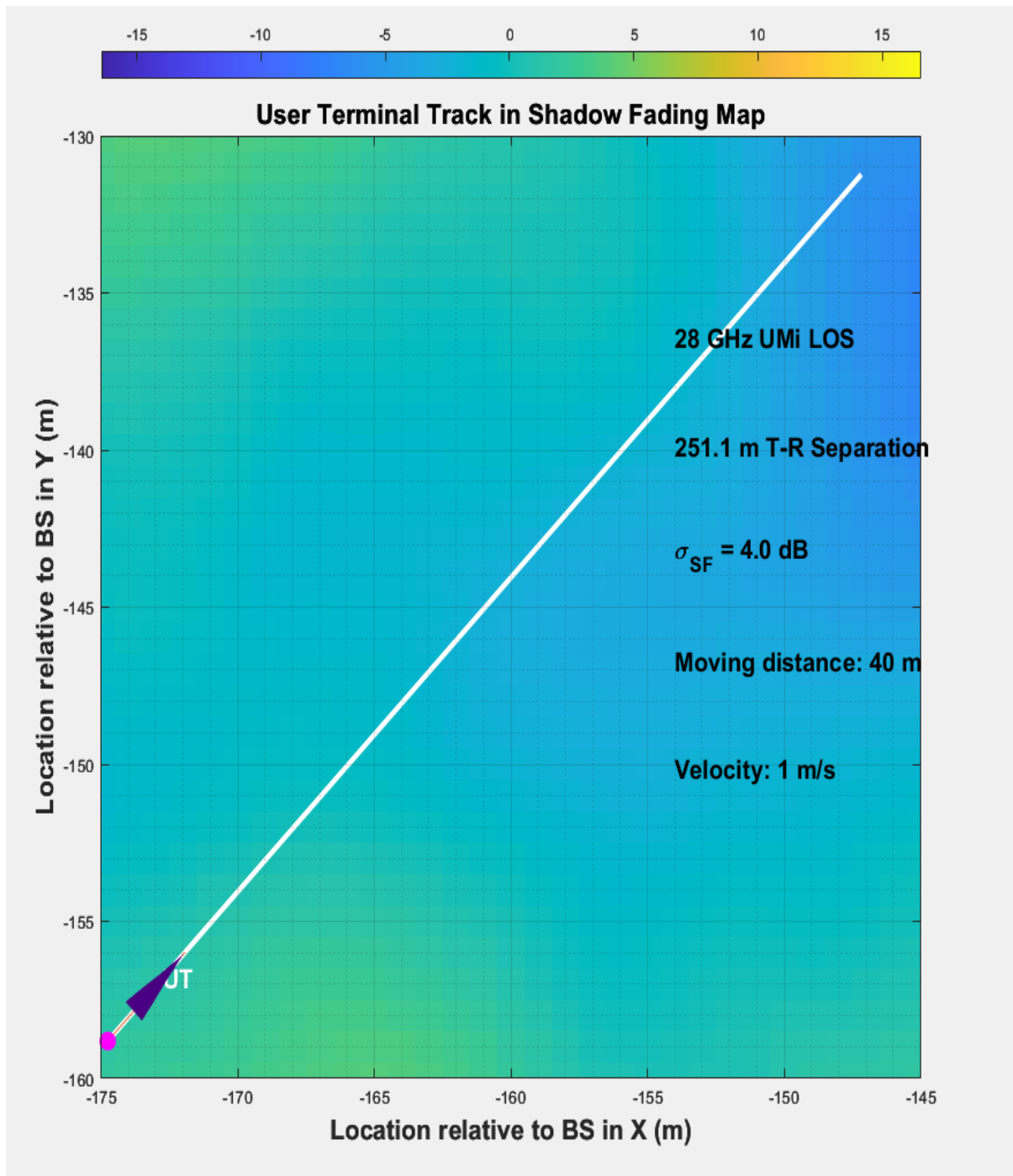


Figure III.14: User terminal track in SF map for scenario 1

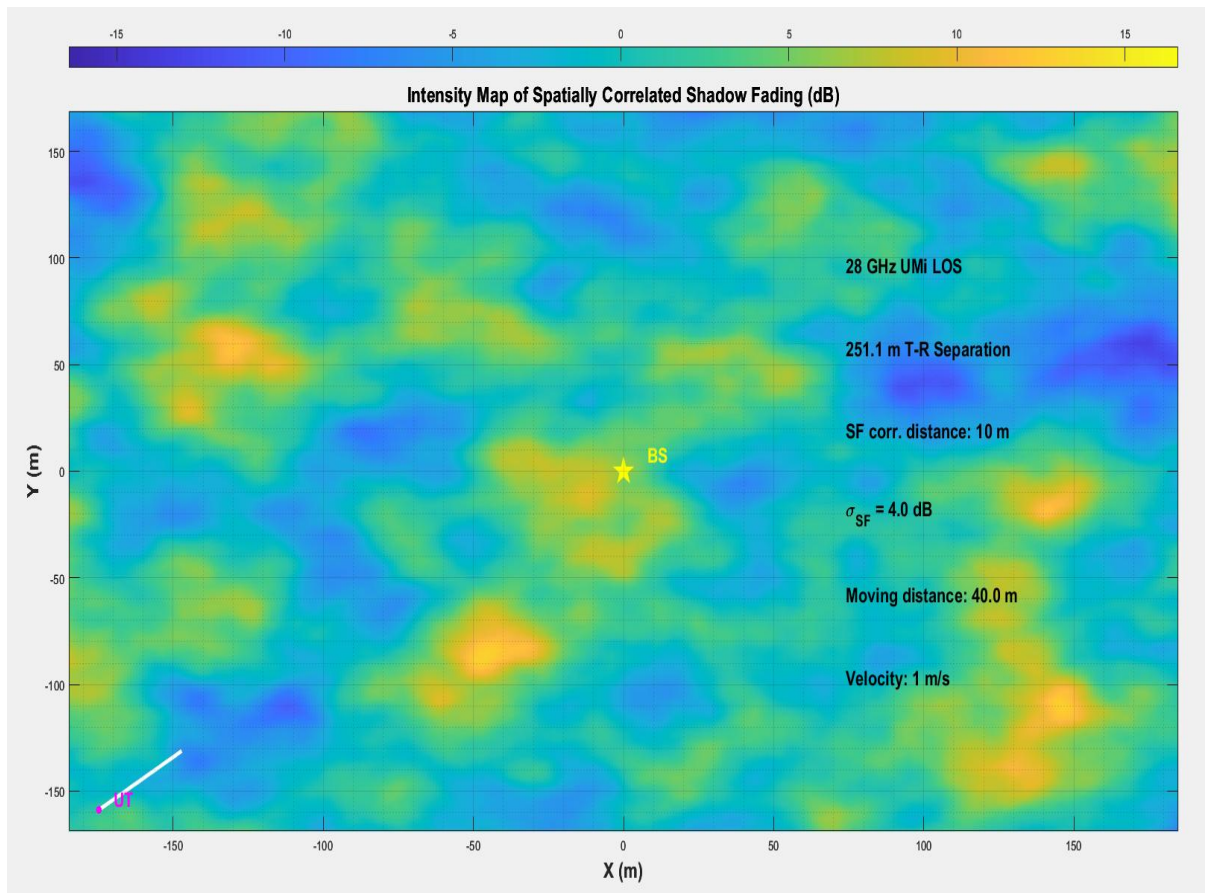


Figure III.15: intensity map of spatially correlated SF for scenario 1

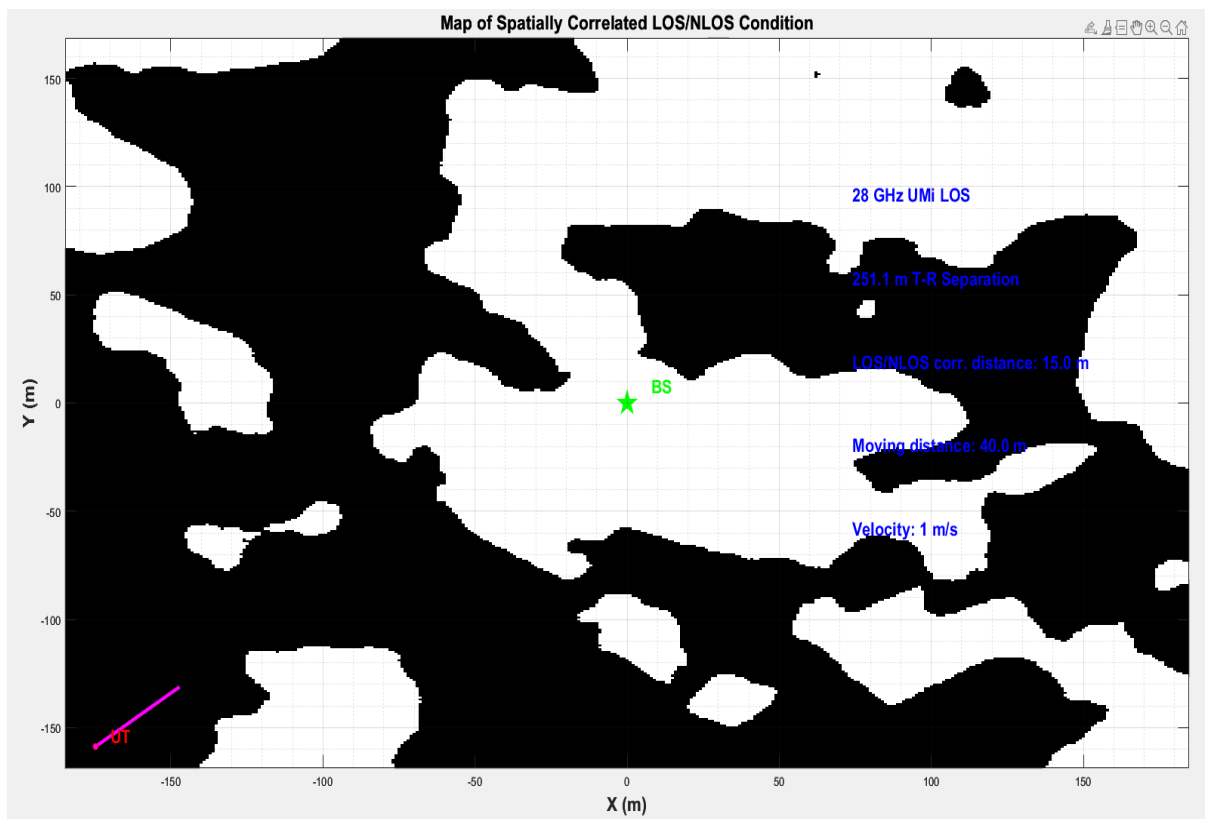


Figure III.16: Map of spatially correlated LOS condition for scenario 1

Table III.3: Observation of scenario one

Graph	Key Observations	Implications
Directional PDP	*Strongest power: -30 to -60dBm * Delay spread: 1500–3000 ns.	*Beamforming mitigates path loss but multipath persists.
Omnidirectional PDP	*Wider power range (-80 to -160 dBm) * Delay spread up to 1600 ns.	*Omnidirectional links suffer higher loss *beamforming is essential.
Shadow Fading Map	*Shadow fading $\sigma_{sF} = 4.0$ dB * Correlation distance: 10 m.	*Consistent large-scale variations impact handover and beam tracking.
LOS/NLOS Map	*LOS/NLOS transitions correlated over 15 m * T-R separation: 251.1 m.	*Blockages (e.g., buildings) cause abrupt link failures.
UT Shadow Fading	*UT movement shows 4 dB fluctuations *Track length: 40 m.	*Real-time beam adaptation needed for mobility.

Commentary: These results capture 5G mmWave’s core tradeoff: directional beamforming enhances link reliability but demands agile tracking to combat real-world variations like shadow fading ($\sigma_{sF}=4$ dB, correlated over 10 m) and abrupt LOS/NLOS transitions. The omnidirectional PDP’s weak power levels (-80 to -160 dBm) underscore mmWave’s harsh propagation limits, while the 10 m shadow fading correlation distance directly impacts beam handover strategies. For reliable deployments, intelligent algorithms must dynamically steer beams and preempt blockages turning mmWave’s raw potential into consistent performance as seen in figure III.3.

III.5.3 Scenario two:

Objective:

This scenario examines the impact of Non-Line-of-Sight (NLOS) conditions on mmWave signal propagation along a linear trajectory. The aim is to understand how beamforming handles severe multipath and signal attenuation in urban NLOS environments.

Table III.4: Parameters used for scenario two

parameter	value
frequency	28(GHz)
Channel Condition	NLOS
Shadow Fading Correlation Distance	10m
Track Type	Linear

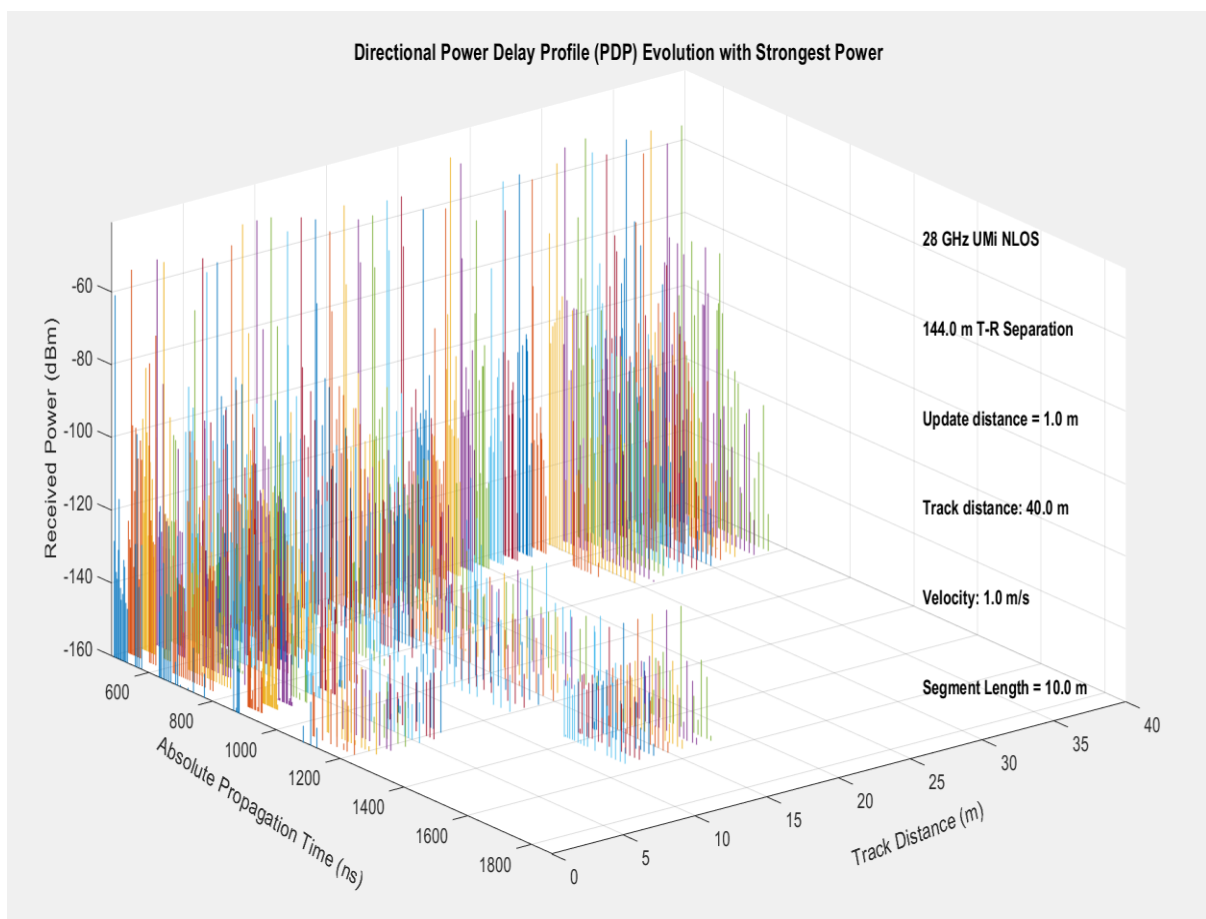


Figure III.17: directional PDP for scenario 2

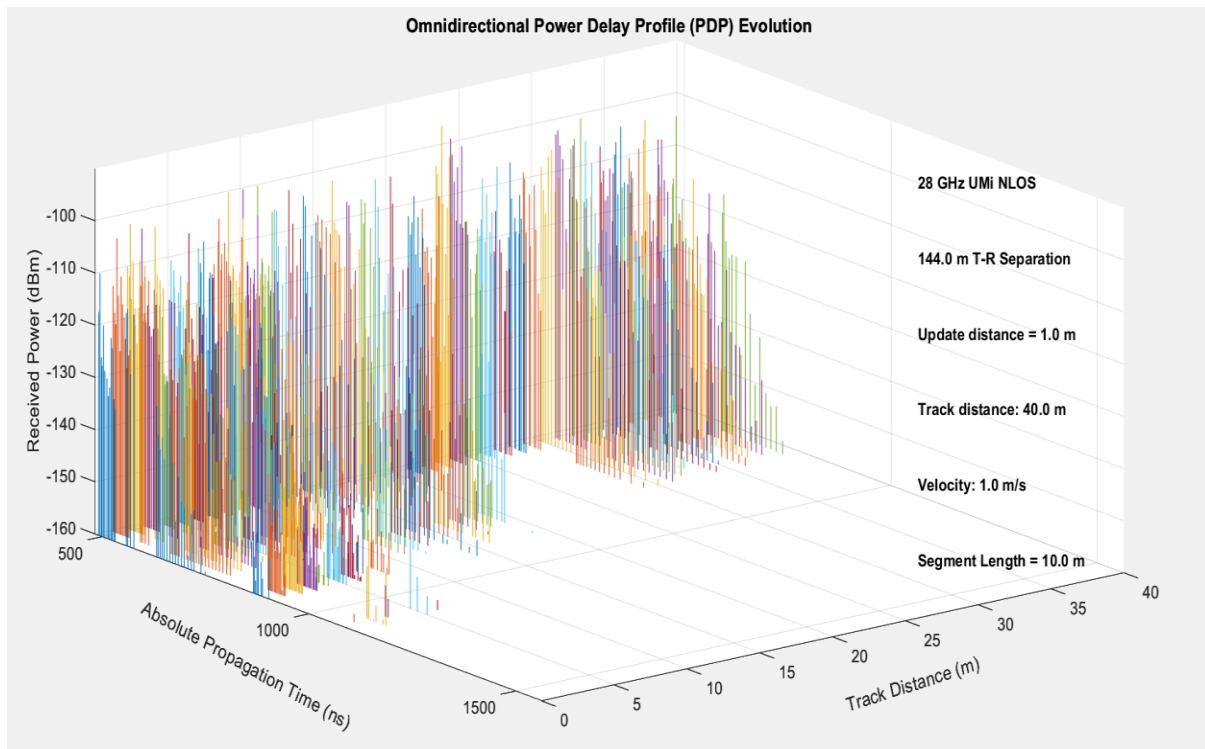


Figure III.18: omnidirectional PDP for scenario 2

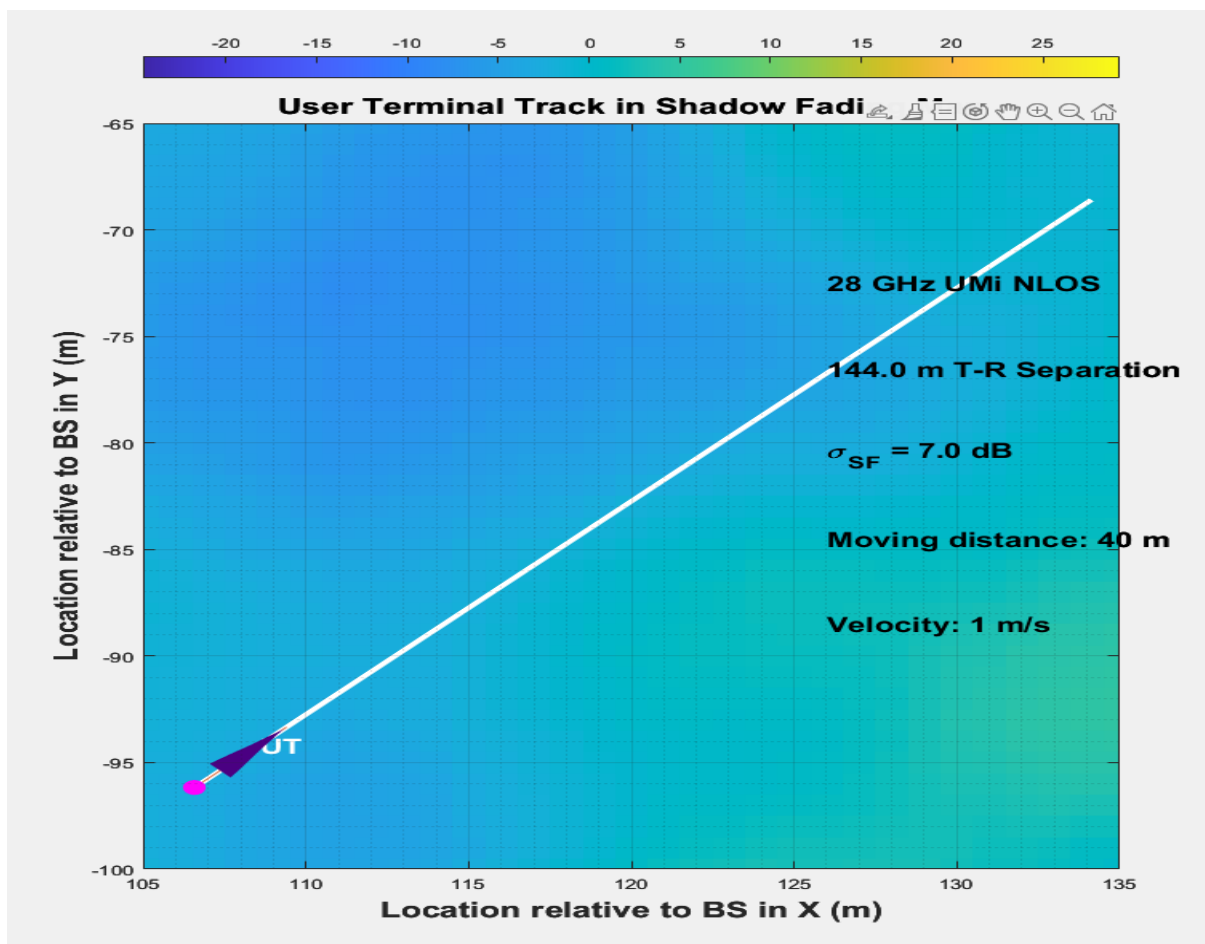


Figure III.19: User terminal track in SF map for scenario 2

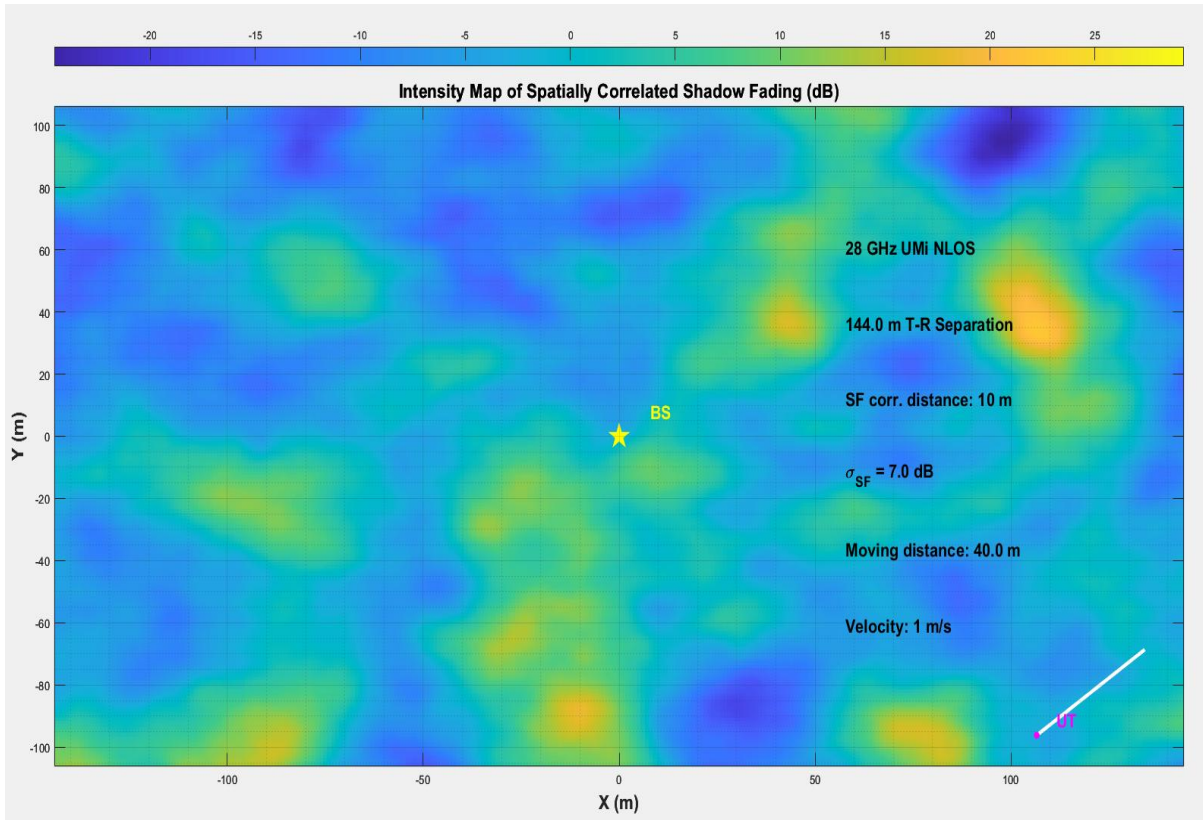


Figure III.20: intensity map of spatially correlated SF for scenario 2

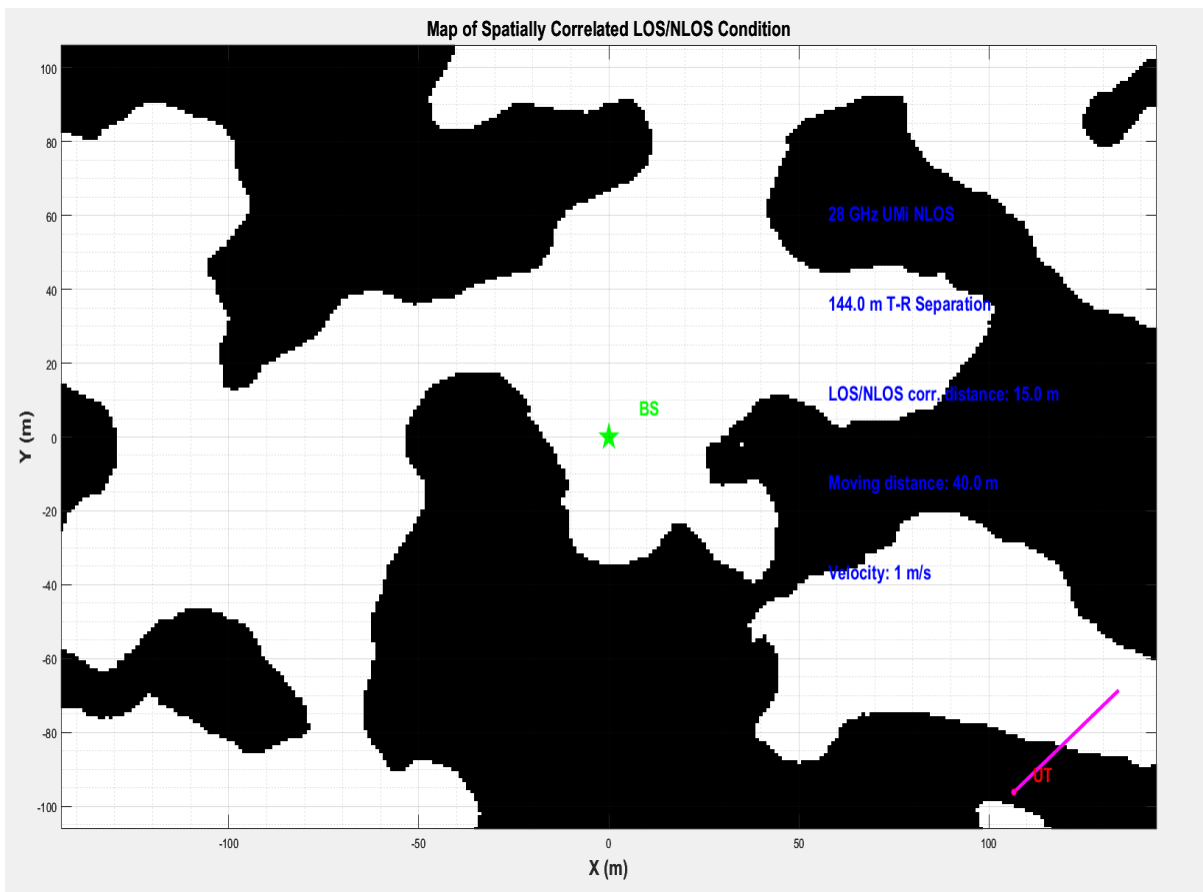


Figure III.21: Map of spatially correlated LOS condition for scenario 2

Table III.5: Observation of scenario two

Graph	Key Findings	Technical Implications
Directional PDP	*Strongest path at -60 dBm * delay spread 800-1800 ns	*Beamforming barely maintains connectivity (-60 dBm) with complex multipath in NLOS
Omnidirectional PDP	*Signal below -100 dBm * undetectable levels	*Confirms omnidirectional mmWave is impractical in NLOS scenarios
LOS/NLOS Map	*15m transition distance * 144m T-R separation	*Blockage patterns remain predictable but challenging at extended NLOS ranges
Shadow Fading Map	* $\sigma_{sF}=7$ dB with 10m correlation	*Strong shadow fading requires robust link margin and frequent beam adjustments
UT Shadow Fading	* ± 35 dB fluctuations over 40m track	*Extreme signal volatility demands real-time beam tracking algorithms

Commentary: The NLOS mmWave simulation results at 144m T-R separation demonstrate significant technical challenges for 5G deployment in urban environments. The directional PDP shows marginal link viability with strongest paths at -60 dBm and substantial delay spread (800-1800 ns), indicating that while beamforming maintains connectivity, it requires advanced equalization techniques. Omnidirectional performance collapses below -100 dBm, proving the necessity of beamforming for NLOS scenarios. The 7dB shadow fading with 10m correlation distance and ± 35 dB fluctuations over 40m movement reveal extreme signal volatility, while the consistent 15m LOS/NLOS transitions highlight predictable but challenging blockage patterns. These findings suggest mmWave networks require ultra-dense cell deployment (≤ 100 m inter-site distance)

III.5.4 Scenario three:

Objective:

This scenario evaluates how turning movements (hexagonal path) influence the spatial behavior of LOS mmWave signals. It helps analyze how angular variations affect directional beam stability and delay spread.

Table III.6: Parameters used for scenario three

parameter	value
frequency	28(GHz)
Channel Condition	LOS
Shadow Fading Correlation Distance	10m
Track Type	Hexagon

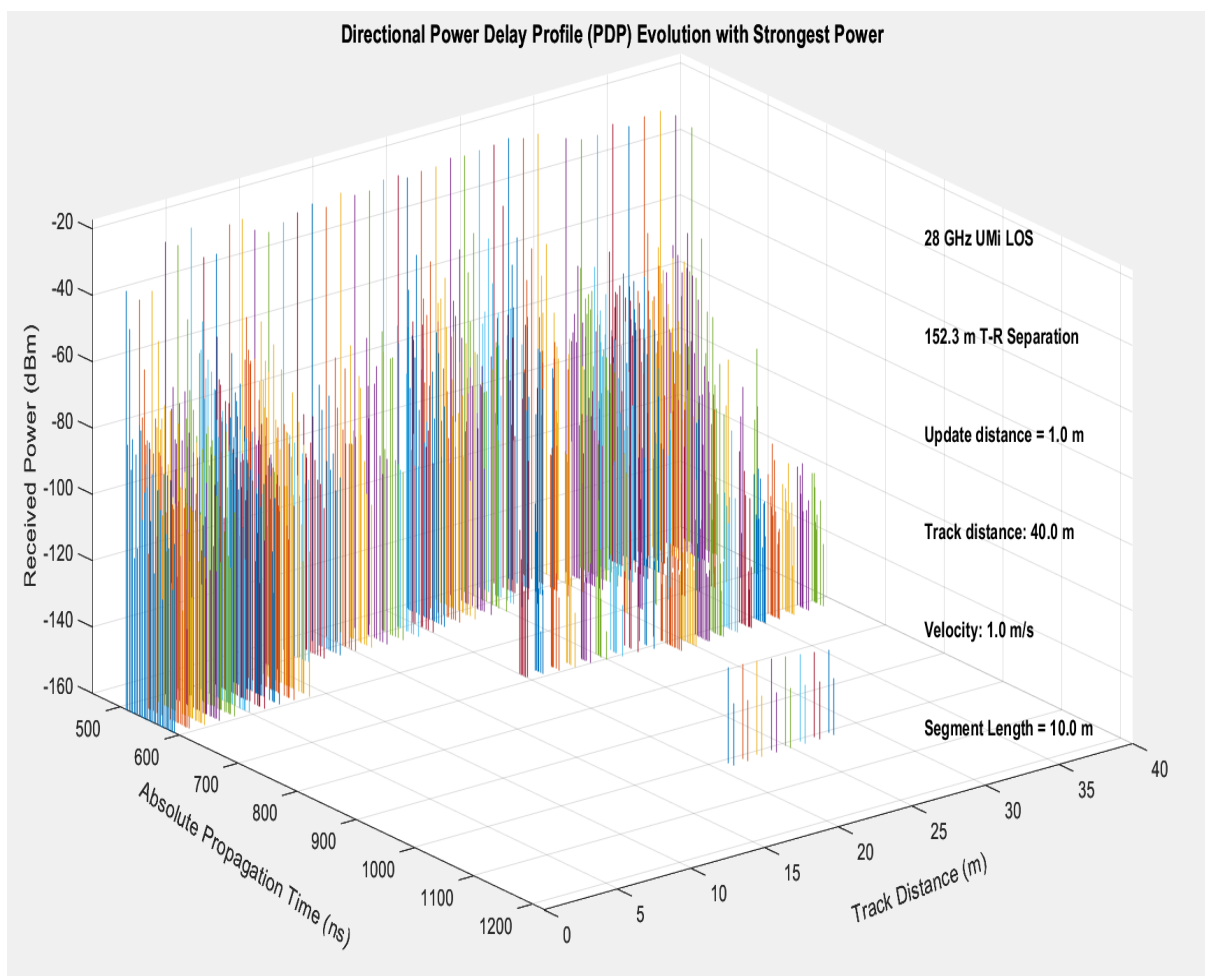


Figure III.22: directional PDP for scenario 3

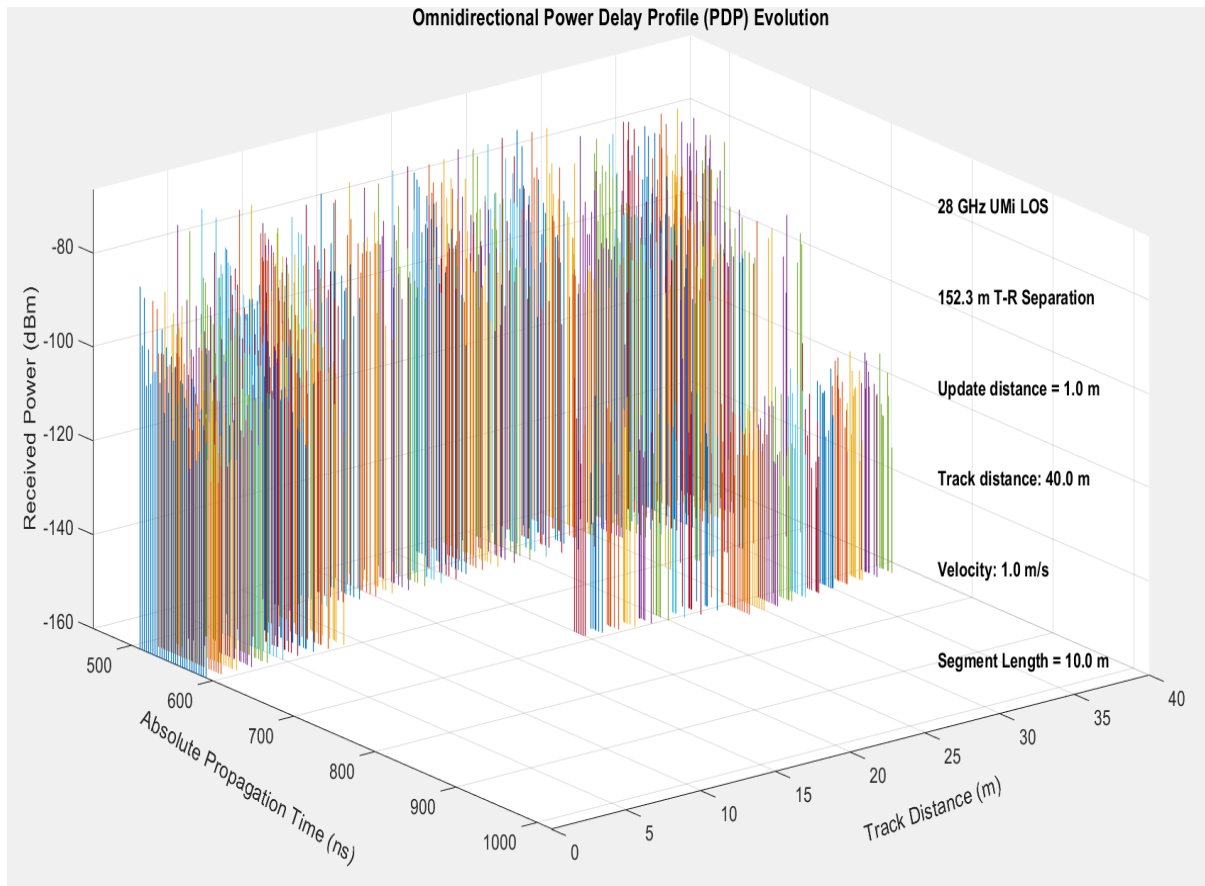


Figure III.23: omnidirectional PDP for scenario 3

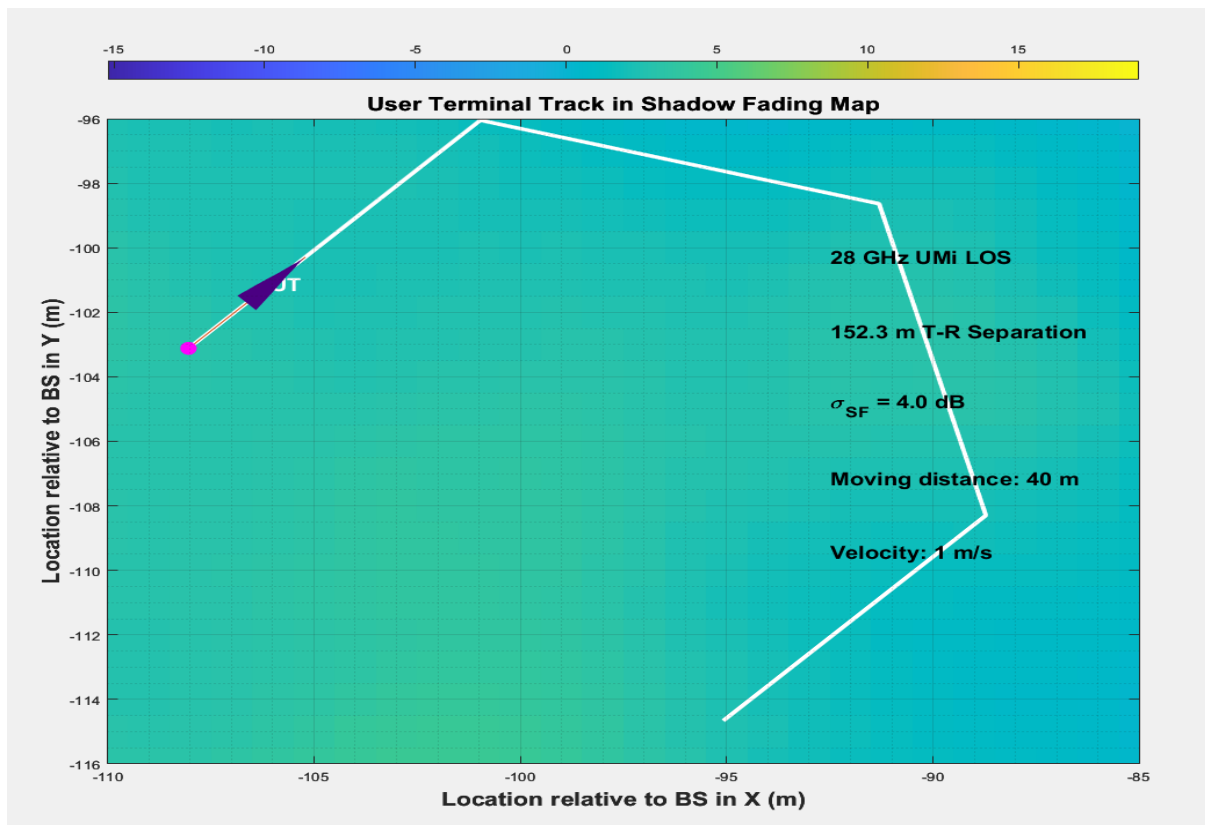


Figure III.24: User terminal track in SF map for scenario 3

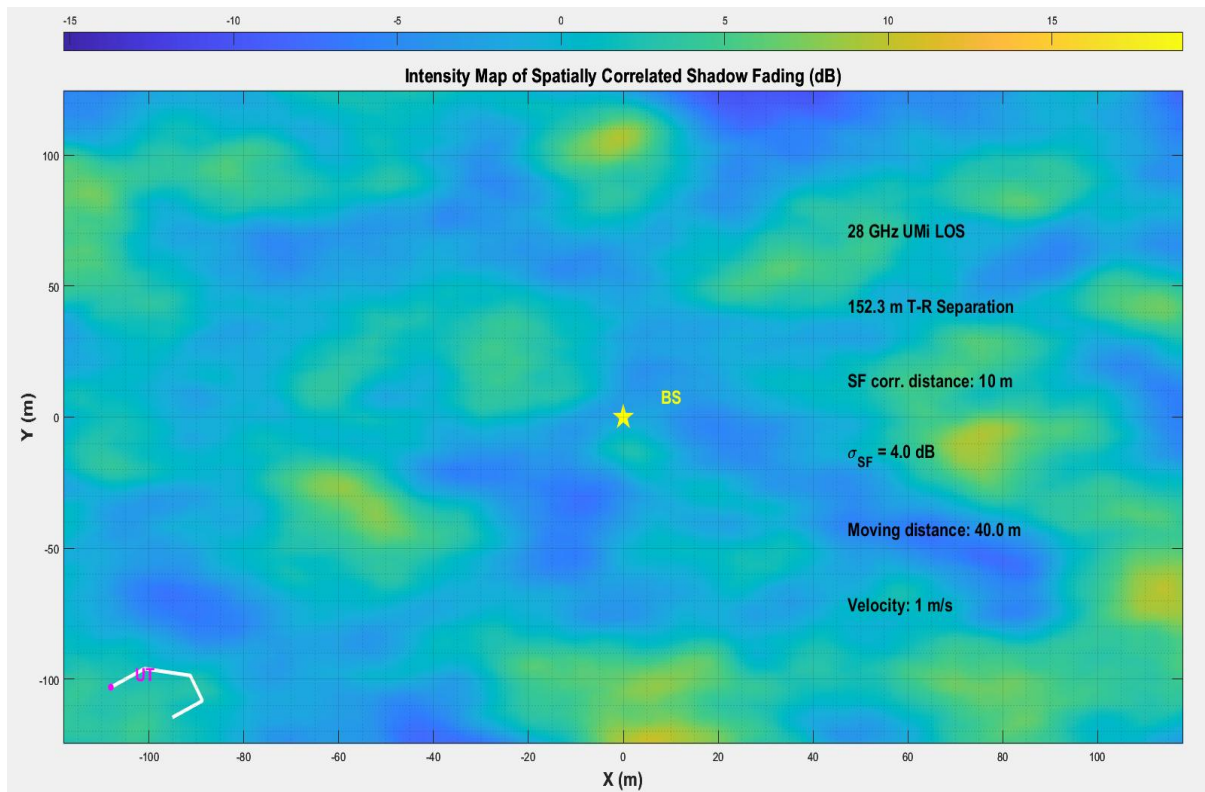


Figure III.25: Intensity map of spatially correlated SF for scenario 3

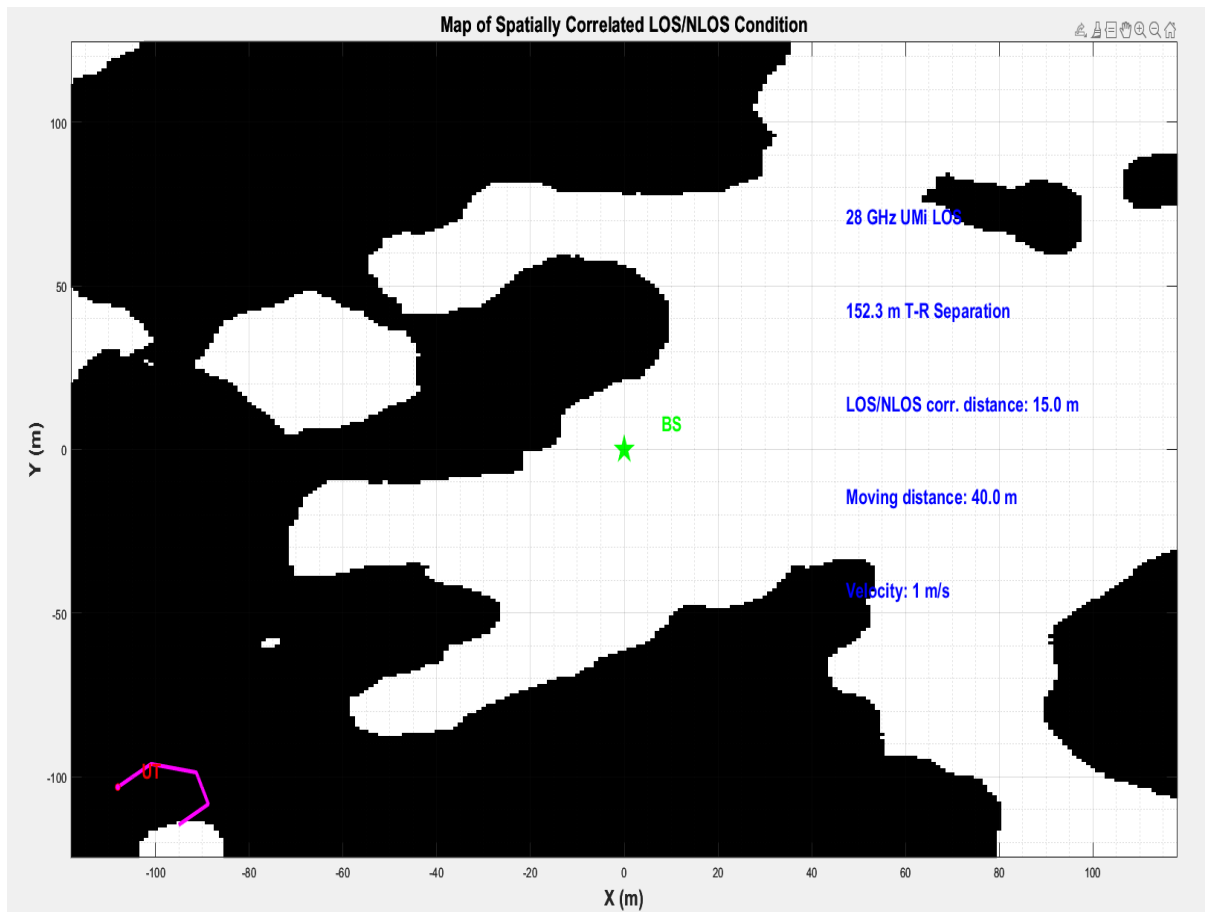


Figure III.26: Map of spatially correlated LOS condition for scenario 3

Table III.7: Observation of scenario three

Graph	Key Findings	Technical Implications
Directional PDP	*Strongest power at -20 dBm * delay spread 500-1600 ns	*Beamforming maintains viable links but requires precise tracking of multipath components
Omnidirectional PDP	*Received power ranges from -80 dBm to -140 dBm *delay spread extends up to ~1600 ns.	*Without beamforming, omnidirectional links result in weak and dispersed signals * highlights the importance of directional antennas in mmWave systems.
LOS/NLOS Map	*15m transition distance *152.3m T-R separation	*Predictable blockage patterns enable proactive beam switching in urban environments
Shadow Fading Map	* $\sigma_s F=4$ dB with 10m correlation distance	*Consistent 10m fading zones demand frequent beam handover strategies
UT Shadow Fading	* ± 15 dB fluctuations over 40m track at 1 m/s	*Real-time beam adaptation crucial for pedestrian mobility scenarios

Commentary: These simulations reveal how mmWave behaves in real urban environments at 152.3m distances. While beamforming maintains a strong -20dBm main path (Directional PDP), the ± 15 dB shadow fading variations (UT Map) show why mmWave is so sensitive to movement - just walking 10m (the correlation distance) can dramatically change signal quality. The 15m LOS/NLOS patterns (LOS/NLOS map) prove that blockages aren't random, but follow urban infrastructure layouts.

III.5.5 Scenario four:

Objective:

This scenario explores the most challenging case: NLOS propagation over a hexagonal user trajectory. It is designed to assess beamforming limitations, path loss, and signal fluctuations in dynamic, obstructed urban mobility conditions.

Table III.8: Parameters used for scenario four

parameter	value
frequency	28(GHz)
Channel Condition	NLOS
Shadow Fading Correlation Distance	10m
Track Type	Hexagon

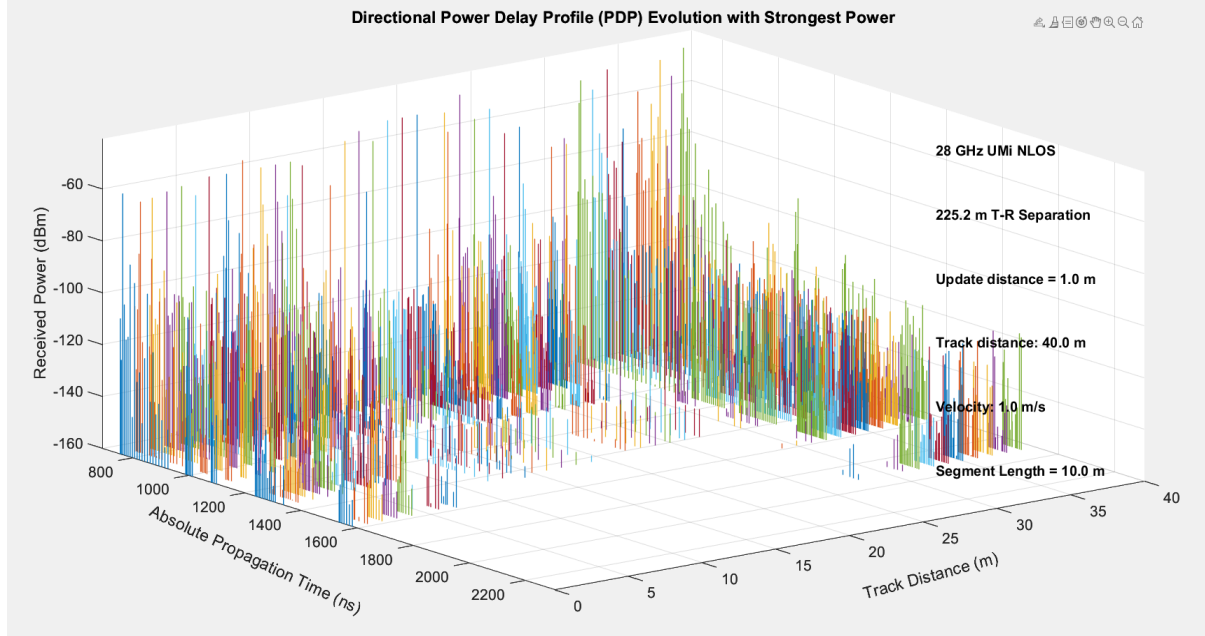


Figure III.27: directional PDP for scenario 4

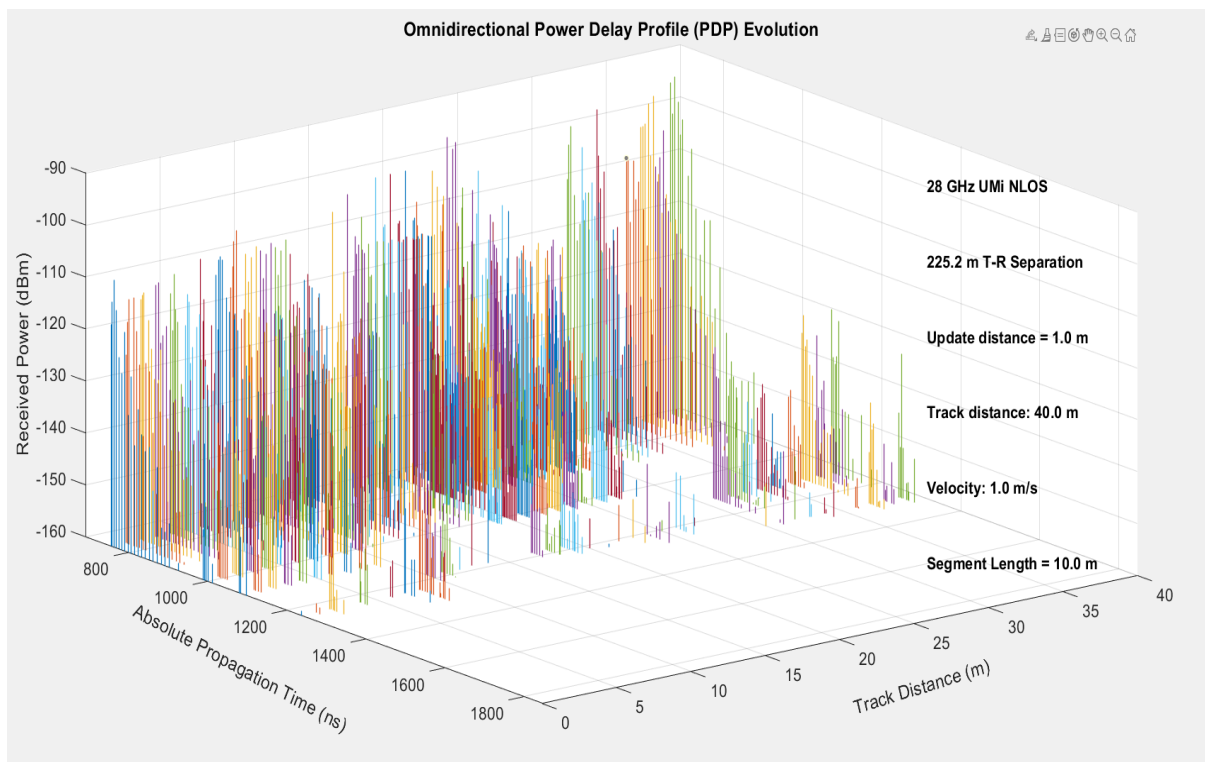


Figure III.28: omnidirectional PDP for scenario 4

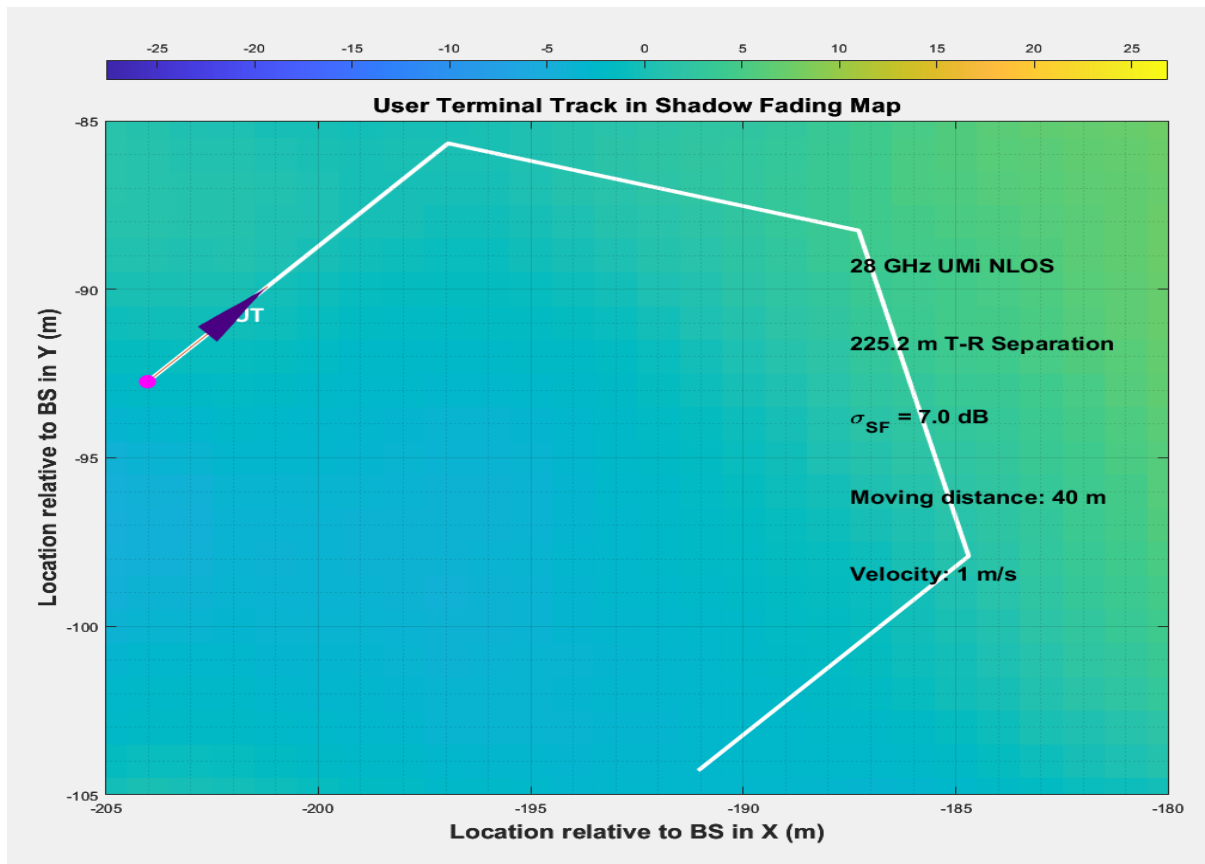


Figure III.28: User terminal track in SF map for scenario 4

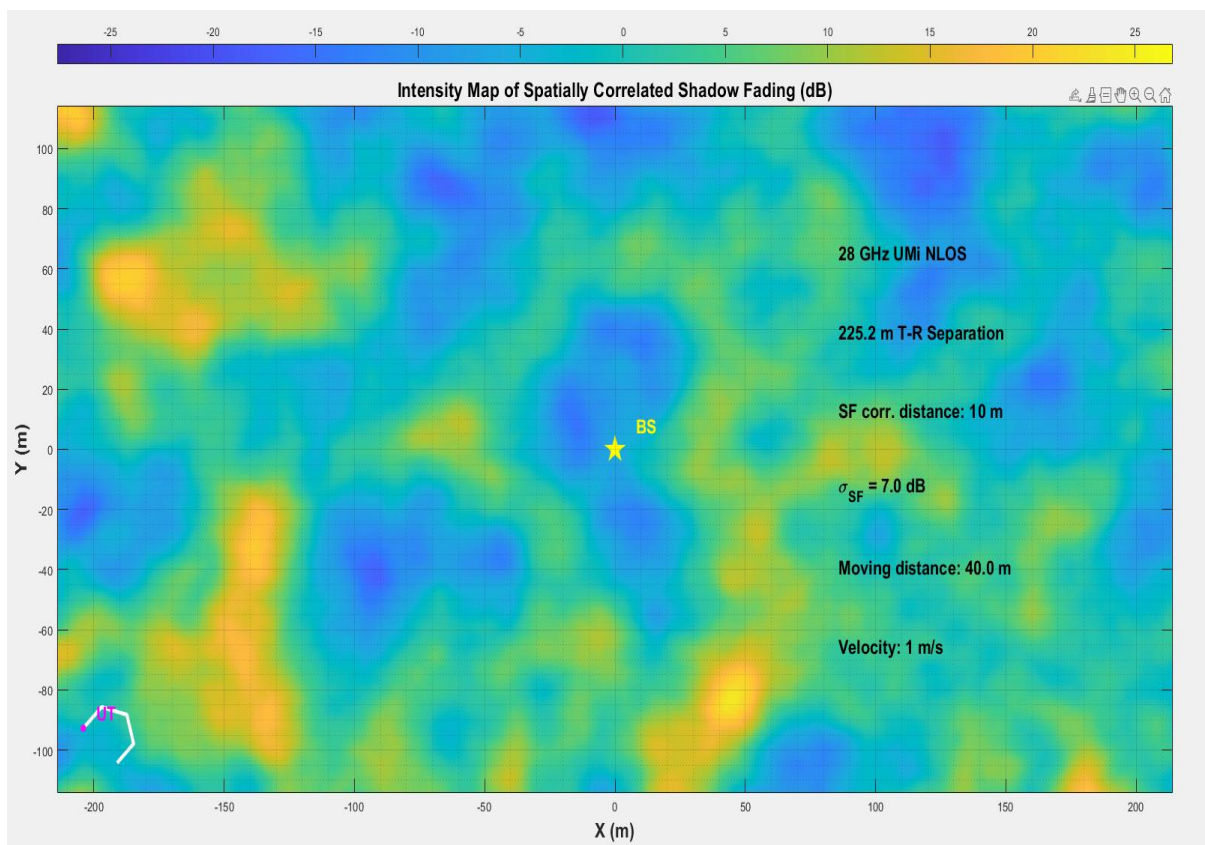


Figure III.29: Intensity map of spatially correlated SF for scenario 4

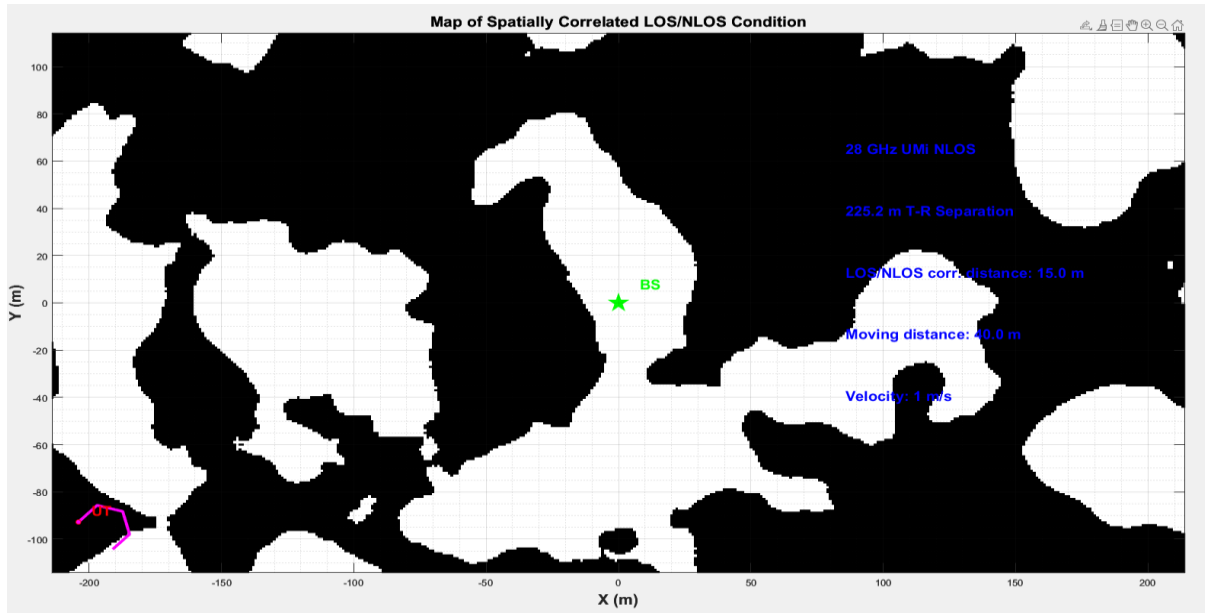


Figure III.30: Map of spatially correlated LOS condition for scenario 4

Table III.9: Observation of scenario four

Graph	Key Findings	Technical Implications
Directional PDP	<ul style="list-style-type: none"> *Strongest power at -60 dBm *delay spread up to 2000 ns 	<ul style="list-style-type: none"> *Severe path loss in NLOS * beamforming barely maintains connectivity at 225.2m
Omnidirectional PDP	<ul style="list-style-type: none"> *Power below -90 dBm * weak signal detection 	<ul style="list-style-type: none"> *Omnidirectional reception fails completely in NLOS conditions
LOS/NLOS Map	<ul style="list-style-type: none"> *15m transition distance * 225.2m T-R separation 	<ul style="list-style-type: none"> *Extended NLOS range challenges mmWave viability *requires repeaters/small cells
Shadow Fading Map	<ul style="list-style-type: none"> *$\sigma_s F = 7$ dB with 10m correlation distance 	<ul style="list-style-type: none"> *Stronger fading (7dB vs 4dB) significantly impacts link reliability
UT Shadow Fading	<ul style="list-style-type: none"> *± 25 dB fluctuations over 40m track at 1 m/s 	<ul style="list-style-type: none"> *Extreme signal variations demand advanced beam tracking algorithms

Commentary: These NLOS simulations at 225.2m reveal mmWave's fundamental limitations: directional beamforming struggles (-60 dBm peak power), omnidirectional links fail completely (<-90 dBm), and 7dB shadow fading creates extreme (± 25 dB) signal variations. The 15m LOS/NLOS correlation distance and 10m fading zones show that urban environments

disrupt mmWave propagation predictably but severely. While beamforming maintains minimal connectivity, these results prove that practical mmWave deployments require: (1) ultra-dense networks (<200m spacing), (2) hybrid sub-6GHz/mmWave architectures for NLOS recovery, and (3) AI-driven beam management that anticipates both 10m fading patterns and 15m blockage transitions.

III.5. 6 Comparative Summary Table:

Table III.10: Comparative Overview of Simulation Outcomes

Parameter / Observation	Scenario1(L OS, Linear)	Scenario2 (NLOS, Linear)	Scenario3 (LOS, Hexagonal)	Scenario 4 (NLOS, Hexagonal)
Shadow Fading Correlation Distance	10 m	10 m	10 m	10 m
T-R Separation Distance	251.1 m	144.0 m	152.3 m	225.2 m
Directional PDP (Peak Power)	-30 to -60 dBm	≈ -60 dBm	≈ -20 dBm	≈ -60 dBm
Omnidirectional PDP (Power Range)	-80 to -160 dBm	< -100 dBm	-80 to -140 dBm	< -90 dBm
UT Shadow Fading Fluctuations	±4 dB	±35 dB	±15 dB	±25 dB
Main Observations	Stable link; beamforming effective	Strong multipath; unstable connectivity	Effective beam tracking; cornering effects	Weak signal; needs dense cells and AI beamforming

Commentary:

This comparison highlights how LOS conditions and beamforming geometry significantly influence signal strength and stability. Scenarios with LOS links and hexagonal tracks show

better performance, while NLOS cases, especially with long T-R separation, suffer from severe fading and weaker received power. Adaptive beam management is crucial for maintaining link quality in dynamic urban environments.

III.6 Simulation without special consistency

To demonstrate the importance of spatial consistency, we ran an additional NYUSIM simulation using the same parameters as before, but with spatial consistency turned off. In this setup, the channel at each position is generated independently, resulting in sudden and unrealistic changes in path loss, shadow fading, and multipath clusters along the user's trajectory. This behavior stands in clear contrast to the smooth, gradual channel evolution seen when spatial consistency is enabled, highlighting why this feature is essential for accurately modeling mobility and beamforming in 5G mmWave systems.

As we can see, simulating without special consistency provides less data and can not be as realistic and accurate as with special consistency.

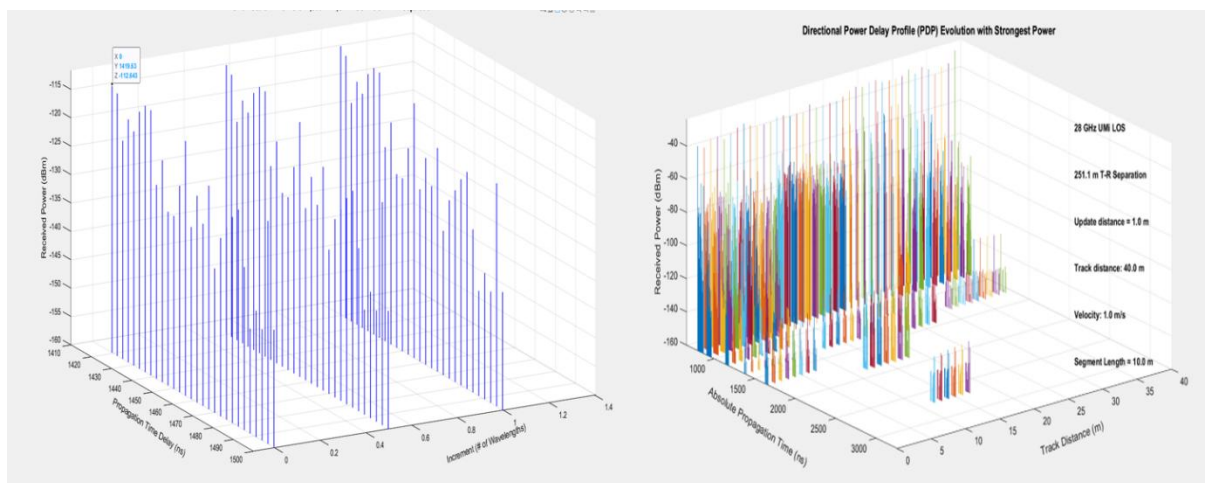


Figure III.31: PDP graphs of simulation without sc and with sc

III.7 Conclusion

In this chapter, we evaluated the impact of spatial consistency parameters on 5G mmWave propagation using the NYUSIM simulator. By varying the shadow fading correlation distance across different track types and channel conditions, we observed how signal behavior changes in both LOS and NLOS environments. The results demonstrate that LOS scenarios benefit significantly from directional beamforming, while NLOS conditions present major challenges due to increased delay spreads and severe signal fluctuations. Hexagonal trajectories introduce additional angular variation, highlighting the importance of adaptive beam steering.

These findings underscore the necessity of dense base station deployment, real-time beam tracking, and robust spatial modeling to ensure reliable mmWave communication in urban 5G networks.

General conclusion

General conclusion

The journey through this thesis has been driven by a central question: how can we realistically model the behavior of 5G wireless channels in motion, particularly in the challenging millimeter-wave (mmWave) bands? As 5G continues to reshape how we live, work, and communicate, the accuracy of our channel models becomes not only a scientific concern but also a practical necessity for engineers, researchers, and network designers alike.

The first chapter introduced us to the foundational concepts of 5G and the revolutionary technologies it brings from ultra-low latency and high-speed connectivity to massive IoT and advanced antenna systems. We saw that while 5G opens new possibilities, it also brings a new layer of complexity in terms of propagation, especially in urban environments where high-frequency signals face severe obstacles such as attenuation, diffraction limitations, and rapid signal fluctuations.

In Chapter II, we shifted our attention to the concept of spatial consistency, a key requirement for ensuring that channel models reflect the gradual and correlated way real-world signals change as users move. We explored the theoretical backbone of this idea and discussed the channel parameters that must evolve smoothly over space: shadow fading, path loss, power delay profiles, and angular information such as angle of arrival (AoA) and departure (AoD). This chapter laid the intellectual foundation for why spatial consistency matters so deeply in the design and optimization of 5G systems.

The final chapter brought theory into practice. Using the NYUSIM simulator, we conducted simulations under carefully selected parameters inspired by real-world conditions in Biskra, Algeria. By varying only the spatial correlation distance and the user's movement pattern, we were able to isolate and analyze the effects of spatial consistency in both LOS and NLOS scenarios. The results were enlightening: while beamforming works remarkably well in LOS conditions, NLOS propagation even with advanced antennas still suffers from sharp signal degradation, increased delay spreads, and unpredictable fading. These findings highlight the importance of adaptive, intelligent network design systems that can track users dynamically, anticipate blockages, and switch beams or frequencies in real-time.

What this thesis ultimately shows is that spatial consistency is not just a mathematical refinement it is a critical factor in building reliable, high-performance 5G systems. Ignoring it

risks designing networks that work perfectly in simulation but fail under real-world mobility. By including it in our models, we step closer to a true understanding of the wireless environment, and a future where 5G performs not just in theory, but in every street, building, and device.

This work provides a foundation upon which future research can build. Further studies might incorporate larger antenna arrays, real-time environmental changes such as weather and foliage, or explore hybrid multi-frequency systems that combine mmWave and sub-6 GHz bands for better robustness. More advanced approaches may also use machine learning to anticipate user behavior and adjust channel parameters dynamically.

In conclusion, this thesis highlights the need for continuous alignment between technological ambition and realistic modeling, reminding us that the real world is never ideal but with the right tools, we can get very close.

References

References

- [1] J. G. Andrews et al., “What Will 5G Be?” *IEEE Journal on Selected Areas in Communications*, vol. 32, no. 6, pp. 1065–1082, Jun. 2014.
- [2] T. S. Rappaport et al., “Millimeter Wave Mobile Communications for 5G Cellular: It Will Work!” *IEEE Access*, vol. 1, pp. 335–349, 2013.
- [3] M. R. Akdeniz et al., “Millimeter wave channel modeling and cellular capacity evaluation,” *IEEE Journal on Selected Areas in Communications*, vol. 32, no. 6, pp. 1164–1179, Jun. 2014.
- [4] T. S. Rappaport et al., “Wireless communications and applications above 100 GHz: Opportunities and challenges for 6G and beyond,” *IEEE Access*, vol. 7, pp. 78729–78757, Jun. 2019.
- [5] G. R. MacCartney and T. S. Rappaport, “A Flexible Millimeter-Wave Channel Simulator for 5G Channel Modeling,” *IEEE Transactions on Antennas and Propagation*, vol. 65, no. 12, pp. 6864–6879, Dec. 2017.
- [6] M. K. Samimi and T. S. Rappaport, “3-D statistical channel model for millimeter-wave outdoor mobile broadband communications,” in *Proc. IEEE Int. Conf. Commun. (ICC)*, May 2016, pp. 1–7, doi: 10.1109/ICC.2016.7511203.
- [7] J. Zhang et al., “Spatial Consistency in 5G Millimeter-Wave Channels: Measurements and Modeling,” *IEEE Transactions on Wireless Communications*, vol. 18, no. 6, pp. 3125–3139, Jun. 2019.
- [8] S. Sun et al., “Investigation of Prediction Accuracy, Sensitivity, and Parameter Stability of Large-Scale Propagation Path Loss Models for 5G Wireless Communications,” *IEEE Transactions on Vehicular Technology*, vol. 65, no. 5, pp. 2843–2860, May 2016.
- [9] A. B. Zekri, R. Ajgou, and E.-H. Meftah, “Effect of Spatial Consistency Parameters on 5G Millimeter Wave Channel Characteristics,” *Progress In Electromagnetics Research B*, vol. 93, pp. 67–85, 2021.
- [10] T. S. Rappaport and S. Deng, “73 GHz Wideband Millimeter-Wave Foliage and Ground Reflection Measurements and Models,” in *Proc. IEEE ICC Workshops*, 2015, pp. 1238–1243.
- [11] H. J. Liebe, G. A. Hufford, and M. G. Cotton, “Propagation modeling of moist air and suspended water/ice particles at frequencies below 1000 GHz,” *AGARD Conf. Proc.*, no. 542, 1993.
- [12] J. J. A. Lempianen, J. K. Laiho-Steffens, and A. F. Wacker, “Experimental results of cross polarization discrimination and signal correlation values for a polarization diversity scheme,” in *Proc. IEEE VTC*, vol. 3, 1997, pp. 1498–1502.

- [13] H. L. Xiao, S. Ouyang, and Z. P. Nie, "The cross polarization discrimination of MIMO antennas at mobile station," in *Proc. Int. Conf. Communications, Circuits and Systems (ICCCAS)*, 2008, pp. 203–206.
- [14] A. A. Saleh and R. A. Valenzuela, "A statistical model for indoor multipath propagation," *IEEE Journal on Selected Areas in Communications*, vol. 5, no. 2, pp. 128–137, Feb. 1987.
- [15] S. Kneifel, A. Battaglia, P. Kollias, M. Maahn, and U. Löhnert, "Ground-based observations of high-frequency microwave attenuation by clouds and precipitation," *Atmospheric Measurement Techniques*, vol. 13, pp. 6559–6575, 2020, doi: 10.5194/amt-13-6559-2020.
- [16] R. Solomon, H. Leung, and E. Hossain, "Analysis of Atmospheric Attenuation in Millimeter-Wave Communication for 5G Applications," *Remote Sensing*, vol. 14, no. 4, p. 946, 2022, doi: 10.3390/rs14040946.
- [17] G. Elgered and P. Jarlemark, "Water vapor radiometry and modeling for satellite communication path attenuation at 22 GHz," *Radio Science*, vol. 55, no. 10, p. e2020RS007093, 2020, doi: 10.1029/2020RS007093.
- [18] A. Aboobaker and S. Zvanovec, "Impact of wet radomes on mmWave signal propagation in non-line-of-sight conditions," *IET Communications*, vol. 12, no. 5, pp. 573–580, 2018, doi: 10.1049/iet-com.2018.5044.
- [19] J. S. Ojo, M. O. Ajewole, and J. A. Ojo, "Radio wave attenuation due to rain and atmospheric gases at Ka-band over Nigeria," in *Modern Spectrum Sharing Techniques and Applications*, T. A. Lomas, Ed., IntechOpen, 2019, doi: 10.5772/intechopen.84221.
- [20] H. C. Nguyen, B. Matthiesen, B. Soret, and K. I. Pedersen, "How important is spatial consistency for realistic mobility-aware channel modeling?" in *Proc. IEEE Globecom Workshops (GC Wkshps)*, Dec. 2018, pp. 1–6, doi: 10.1109/GLOCOMW.2018.8644366.
- [21] 3GPP TR 38.901 V16.1.0, "Study on channel model for frequencies from 0.5 to 100 GHz," Dec. 2020. [Online]. Available: https://www.3gpp.org/ftp/Specs/archive/38_series/38.901/
- [22] 3GPP TS 23.501, "System Architecture for the 5G System," Release 17, 2022.
- [23] ETSI, "5G Use Cases in Smart Cities," [Online]. Available: <https://www.etsi.org>
- [24] 5G.co.uk, "What is 5G? The Next Generation Mobile Network Explained," [Online]. Available: <https://5g.co.uk>
- [25] Evercom Communication Technology Co., Ltd., "Understanding of SISO, SIMO, MISO and MIMO," [Diagram], Sep. 2019. [Online]. Available: <https://www.evercomtech.com/understanding-isis-simo-miso-mimo>

-
- [26] Qorvo. (n.d.). Base station types [Image]. Qorvo Design Hub. Retrieved from <https://www.qorvo.com/design-hub/blog/small-cell-networks-and-the-evolution-of-5g>
- [27] S. Bakri, "Towards Enforcing Network Slicing in 5G Networks," Master's thesis, Sorbonne University, France, 2021.
- [28] R. L. Smeliansky, "Hierarchical Edge Computing," in *Proc. of IEEE INFOCOM 2018 – IEEE Conference on Computer Communications*, Honolulu, HI, USA, Apr. 2018
- [29] A. F. Molisch, *Wireless Communications*, 2nd ed., Wiley-IEEE Press, 2011.
- [30] T. S. Rappaport, *Wireless Communications: Principles and Practice*, 2nd ed., Prentice Hall, 2014.
- [31] E. Dahlman, S. Parkvall, and J. Skold, *5G NR: The Next Generation Wireless Access Technology*, Academic Press, 2016
- [32] The MathWorks, Inc. (n.d.). *Interactive CDL channel model configuration and visualization*. <https://www.mathworks.com/help/5g/ug/interactive-cdl-channel-model-configuration-and-visualization.html>
- [33]The MathWorks, Inc. (n.d.). *WINNER II channel*.<https://www.mathworks.com/help/comm/ug/winner-ii-channel.html>
- [34] Auden Techno Corp. (n.d.). *RLS-2100 satellite radio link emulator*. https://www.auden.com.tw/en/es_biz/rls-2100-satellite-radio-link-emulator/
- [35] Remcom. (n.d.). *Remcom announces new version of Wireless InSite with engineered electromagnetic surface modeling*. <https://www.remcom.com/press-releases/remcom-announces-new-version-of-wireless-insite-with-engineered-electromagnetic-surface-modeling>

